Environmental Science & Technology

Critical Review

pubs.acs.org/est

Metal Stable Isotope Signatures as Tracers in Environmental Geochemistry

Jan G. Wiederhold*[†,‡]

[†]Soil Chemistry Group, Institute of Biogeochemistry and Pollutant Dynamics, ETH Zurich, 8092 Zurich, Switzerland

[‡]Isotope Geochemistry Group, Institute of Geochemistry and Petrology, ETH Zurich, 8092 Zurich, Switzerland

Supporting Information

ABSTRACT: The biogeochemical cycling of metals in natural systems is often accompanied by stable isotope fractionation which can now be measured due to recent analytical advances. In consequence, a new research field has emerged over the last two decades, complementing the traditional stable isotope systems (H, C, O, N, S) with many more elements across the periodic table (Li, B, Mg, Si, Cl, Ca, Ti, V, Cr, Fe, Ni, Cu, Zn, Ge, Se, Br, Sr, Mo, Ag, Cd, Sn, Sb, Te, Ba, W, Pt, Hg, Tl, U) which are being explored and potentially applicable as novel geochemical tracers. This review presents the application of metal stable isotopes as source and process tracers in environmental studies, in particular by using mixing and Rayleigh model approaches. The most important concepts of mass-dependent and mass-independent metal stable isotope fractionation are introduced, and the extent of natural isotopic variations for different elements is compared. A particular focus lies on a discussion of processes (redox transformations, complexation, sorption, precipitation, dissolution, evaporation, diffusion, biological cycling) which are able to induce metal stable isotope fractionation in environmental systems. Additionally, the usefulness and limitations of metal stable isotope signatures as tracers in environmental geochemistry are discussed and future perspectives presented.

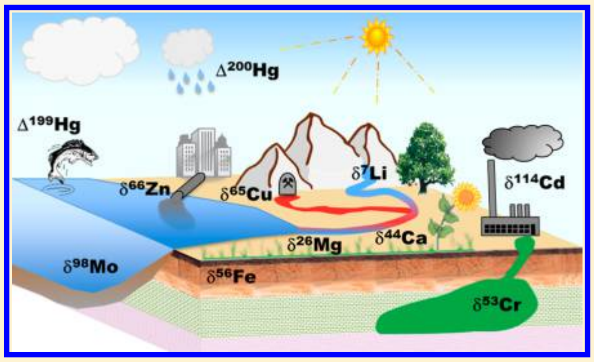

■ INTRODUCTION

Stable isotope ratios of chemical elements in environmental samples contain valuable information on sources and processes which have influenced the history of the samples. Stable isotope analysis of light elements (H, C, O, N, S) has been successfully applied for many decades to study their environmental cycling in many different settings and to address a variety of basic and applied problems in environmental geochemistry.[1−3] These so-called "traditional" stable isotope systems encompass only elements which can be conveniently converted into a gaseous form and analyzed by gas-source mass spectrometers.[4] A lack of suitable techniques to resolve natural variations in the stable isotope composition of heavier elements, especially metals, prevented further progress for a long time. Analytical developments and methodological improvements over the last two decades have now expanded the feasibility of high-precision stable isotope analyses to almost the entire periodic table and thereby triggered the development of a new scientific field. This review provides an overview of the rapidly growing research area of metal stable isotope geochemistry, with a particular focus on applications in environmental geochemistry. This includes primarily the present-day cycling of metals and metalloids in the environment related to their important roles (1) as integral components of earth surface processes (e.g., weathering, pedogenesis), (2) as nutrients for organisms (e.g., plants, microorganisms), and (3) as pollutants affecting natural ecosystems as a result of anthropogenic activities (e.g., emissions from industrial or mining sources). In consequence, other applications of metal stable isotopes such as in high-temperature geochemistry[5] or low-temperature geochemical studies focusing on the evolution of the Earth on geological time scales[6] are not targeted here.

A first comprehensive review was provided in 2004 with the volume *Geochemistry of Non-Traditional Stable Isotopes*, edited by Johnson, Beard, and Albarède,[7] containing an excellent introduction into the relevant fundamental concepts, analytical aspects, and theoretical predictions, as well as pioneering review chapters on ten elements (Li, Mg, Cl, Ca, Se, Cr, Fe, Cu, Zn, Mo). The potential application of metal stable isotope ratios to study sources and fate of metals in the environment was presented in a feature article in 2008 by Weiss et al.[8] The topic was further introduced in the *Elements* focus issue "*Metal Stable Isotopes − Signals in the Environment*" edited by Bullen and Eisenhauer[9] in 2009. Another milestone was the publication of the *Handbook of Environmental Isotope Geochemistry* edited by Baskaran[10] in 2012, containing chapters focusing on novel stable isotope systems (Li, Si, Ca, Cd, Cr, Se, Hg, Tl) and an

Received: September 24, 2014
Revised: January 30, 2015
Accepted: February 1, 2015
Published: February 2, 2015

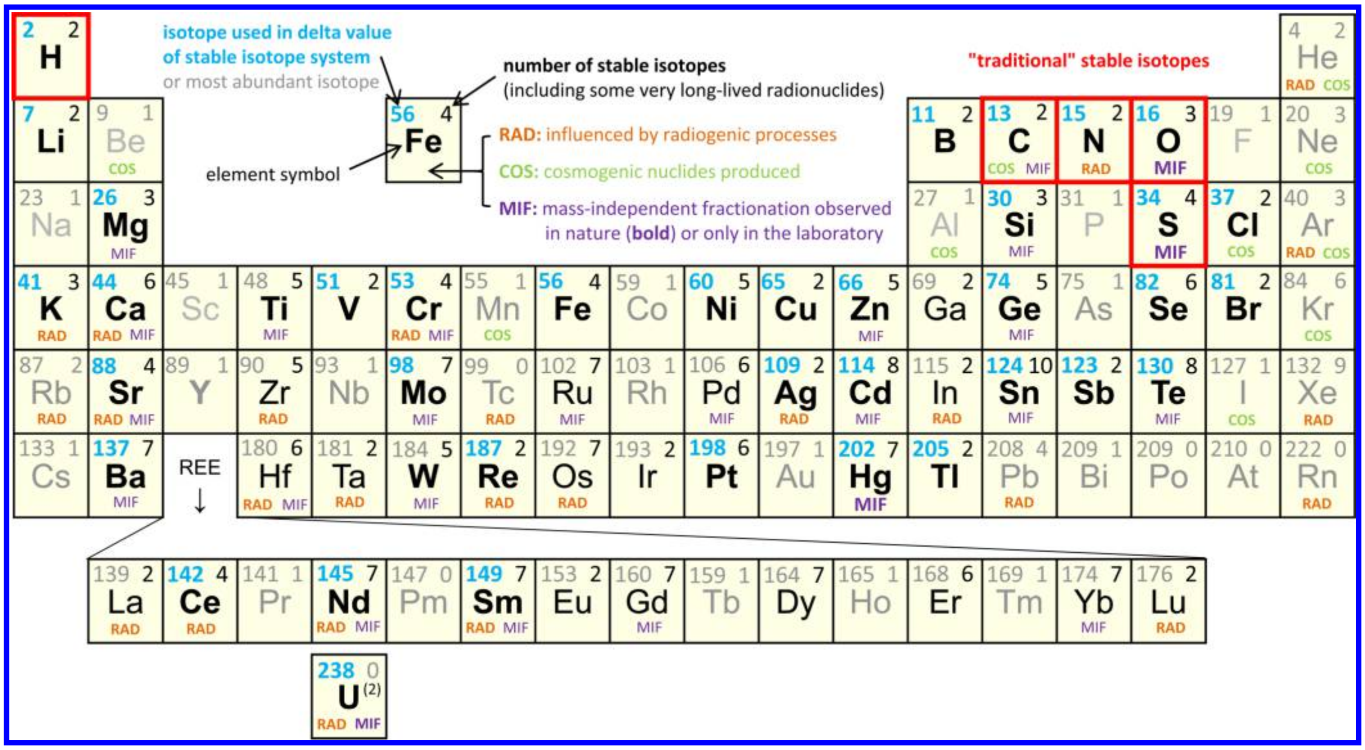

Figure 1. Periodic table with selected elemental properties relevant for stable isotope research. Indicated are the number of stable isotopes of an element (upper right corner), the mass of the isotope commonly used in the delta value or alternatively the most abundant isotope (upper left corner), and the potential influence of radiogenic (RAD) and cosmogenic processes (COS) as well as mass-independent fractionation (MIF) on the stable isotope system (below the element symbol). In most cases, MIF due to nuclear volume[41] or magnetic isotope effects[63] (see section "Mass-Independent Fractionation (MIF)") has only been observed in laboratory-scale studies and has not yet been detected in natural samples (except for O, S, and Hg, marked in bold). The "traditional" stable isotope systems are marked with a red border. Elements for which high-precision stable isotope methods have been developed are marked with a bold symbol. The actinides possessing no stable isotopes are not included (except for U with two long-lived radionuclides exhibiting stable isotope fractionation). Please see SI Table S1 for details on individual elements.

overview chapter by Bullen[11] summarizing the state of research and outlining potential applications for transition and post-transition metal isotopes in environmental studies. Additional recent reviews present applications of metal stable isotopes in weathering and hydrology[12] and other environmental systems.[13−16]

Building upon the material presented in those previous reviews and incorporating the findings of more recent studies, this contribution aims to provide an overview on the current state of research on environmental applications of metal stable isotope geochemistry. In the first section, fundamental concepts of stable isotope geochemistry and the nomenclature used for data reporting are presented. The second section introduces different types of stable isotope fractionation, including mass-independent effects which had not been covered in previous reviews. It also gives an overview of natural stable isotope variations of elements across the periodic table, revealing their close link to the geochemical properties and environmental behavior of an element. In the third section, the application of metal stable isotope signatures as tracer for sources and processes in environmental geochemistry and the most important model approaches are presented. Afterward, processes causing metal isotope fractionation (redox transformations, complexation, sorption, precipitation, dissolution, evaporation, diffusion, biological cycling) are discussed in individual subsections. Finally, the applicability of metal stable isotopes as tracers in environmental geochemistry is discussed, and future perspectives are presented. Additionally, a short description of analytical techniques for metal stable isotopes and an overview of the current state of research on individual elements is provided as Supporting Information (SI).

Stable Isotope Basics. Isotopes are atoms of an element with different numbers of neutrons and thus different masses. They behave very similarly in most chemical reactions, which are governed by the nuclear charge, defined by the number of protons, and the configuration of the outer electron shells. However, the different masses cause slight differences in reactivity and physicochemical properties between isotopes of an element (see section "Fractionation of Stable Isotopes"). Most elements in the periodic table (Figure 1) consist of mixtures of multiple stable isotopes, with their weighted average determining the atomic mass. For instance, copper consists of two stable isotopes (^{63}Cu, ^{65}Cu) with relative abundances of 69.2% and 30.8%, resulting in an atomic mass of 63.546 g mol^{-1}. Only 21 elements consist of only one stable isotope. The environmental cycling of these monoisotopic elements cannot be investigated by stable isotope fractionation studies, which is unfortunate because some of them play important roles in biogeochemical cycles (e.g., Na, Al, P, Mn, As). However, all other elements consist of mixtures of two or more stable isotopes (up to 10) which potentially allows deducing information about their environmental cycling from stable isotope variations. The fundamental reasons why certain elements possess multiple stable isotopes and in which abundance are related to nucleosynthetic constraints. The initial formation of elements and their isotopes occurred at the beginning of the universe and during subsequent stellar nuclear fusion and decay processes.[17] This topic lies outside the scope

DOI: 10.1021/es504683e
Environ. Sci. Technol. 2015, 49, 2606−2624

of this review, but a useful rule of thumb related to fundamental symmetry principles in nucleosynthesis predicts that elements with even atomic numbers tend to have more stable isotopes than elements with odd atomic numbers, and within stable isotopes of an element, isotopes with even masses tend to be more abundant than those with odd masses.[1]

Different Origins of Metal Isotope Variations. This review discusses variations in stable isotope compositions of metals and metalloids caused by fractionating processes. However, metal stable isotope variations of some elements can also be caused by radiogenic processes, that is, the radioactive decay of unstable to stable isotopes. The most important examples for environmental studies are strontium (Sr) and lead (Pb),[18] both possessing four stable isotopes. For Sr, one isotope is influenced by radiogenic processes (^{87}Rb−^{87}Sr decay) whereas the other three are only influenced by stable isotope fractionation (e.g., ^{88}Sr/^{86}Sr), enabling the use of Sr isotope signatures as two-dimensional tracer by investigating radiogenic processes and stable isotope fractionation in parallel.[12] While radiogenic Sr isotope variations have been studied for many decades and applied in many fields such as ecosystem research,[19] the study of natural waters,[20] and archeology,[21] the study of stable Sr isotope fractionation is still in its infancy. For Pb, three of the four stable isotopes are end products of radioactive U−Th decay chains. Therefore, stable Pb isotope fractionation cannot be detected in natural samples, because there is no ratio between two isotopes which is not influenced by radiogenic processes. Depending on geochemical composition and age of source materials, relatively large Pb isotope variations can be observed between environmental samples and these are generally believed to overwhelm potentially occurring mass-dependent and nuclear-volume (see section "Nuclear Volume Effect (NVE)") effects of Pb isotopes by a factor of up to 200.[22] Radiogenic Pb isotope variations have been studied extensively, for instance for environmental source tracing.[23] Elements influenced by radiogenic processes (both as parent or daughter) are marked in Figure 1 ("RAD"). Cosmogenic processes in the atmosphere produce short-lived nuclides of some elements ("COS" in Figure 1) which may be used to study earth surface processes[24] (e.g., ^{10}Be, ^{26}Al) and for dating purposes (e.g., ^{14}C). Some radioactive metal isotopes are produced by natural (e.g., ^{210}Pb[25]) and anthropogenic nuclear processes (e.g., ^{137}Cs). Finally, metal stable isotopes used as enriched tracers ("spikes") offer many applications in environmental studies,[26−29] but these are also not a topic of this review focusing on metal isotope variations caused by fractionating processes.

Stable Isotope Nomenclature. Stable isotope variations are reported as relative values compared with reference materials. This has analytical reasons because absolute isotope ratios are more difficult to measure with high precision and accuracy. Additionally, it is essential that results of different laboratories can be related to each other, which requires defining common reference materials as "zero baseline" for isotopic analyses of elements. Therefore, stable isotope data are expressed as delta values (δ) by normalizing isotope ratios in samples to the ratio of a standard material (eq 1),

$$\delta^{x}E = \frac{(^{x}E/^{y}E)_{\text{sample}}}{(^{x}E/^{y}E)_{\text{standard}}} - 1 \tag{1}$$

where x and y represent isotopes of the element E. Because the resulting values are usually small, delta values are expressed in parts per thousand by multiplying with 1000 and adding the permil sign (‰). However, this factor should not be part of the delta value definition according to recent IUPAC recommendations.[30] Only the heavier isotope is commonly included in delta values (e.g., δ^{65}Cu to describe the ^{65}Cu/^{63}Cu ratio) except when it is unclear which ratio is referred to (e.g., δ^{44}Ca), in which case both isotopes can be included in the delta value (e.g., $\delta^{44/40}$Ca or $\delta^{44/42}$Ca). Importantly, stable isotope ratios are expressed with heavy isotopes in the numerator and light isotopes in the denominator ("heavy over light"). Thus, positive values indicate relative enrichments of heavy isotopes and negative values relative enrichments of light isotopes compared with the reference material possessing a value of 0‰. Samples are often denoted as "isotopically heavy" or "isotopically light", but it must always be clarified which baseline is used for comparison (e.g., another sample or standard material).

The fractionation between two compounds is often expressed with the fractionation factor alpha (α) (eq 2), defined as the ratio of the isotope ratios in the compounds,

$$\alpha_{A-B} = \frac{^{x/y}R_{\text{A}}}{^{x/y}R_{\text{B}}} \tag{2}$$

where R is the ratio of the isotopes x and y in compounds A and B. Since alpha values are usually numbers close to unity, it is convenient to express the extent of fractionation between two samples with the enrichment factor epsilon (ε) (eq 3),

$$\varepsilon_{\text{A-B}} = \alpha_{\text{A-B}} - 1 \tag{3}$$

which is multiplied with the factor 1000 and reported in permil (‰), similar to delta values. A convenient approximation (eq 4), valid for delta values <10‰,[1] relates the parameters ε, δ, and α (for ε and δ expressed in permil):

$$\varepsilon_{\text{A-B}} \approx \delta_{\text{A}} - \delta_{\text{B}} \approx 1000 \ln \alpha_{\text{A-B}} \tag{4}$$

The symbol epsilon has also been used in some studies to describe isotopic differences in parts per ten thousand, but this is not in accordance with IUPAC recommendations.[30]

For elements with more than two stable isotopes, the relative extent of fractionation between isotopes can usually be predicted by simple mass-dependent relationships. For instance, the fractionation of ^{48}Ca relative to ^{40}Ca is a factor of about 8 larger than fractionation between ^{43}Ca and ^{42}Ca. Approximate scaling factors inferred from the mass difference are sufficient in most cases. Otherwise, precise scaling factors beta (β) describing the relationship between fractionation factors (eq 5),

$$\alpha_{2/1} = (\alpha_{3/1})^{\beta} \tag{5}$$

where 1, 2, and 3 represent different isotopes of an element, can be derived from mass-dependent kinetic and equilibrium fractionation laws[31] (eqs 6 and 7),

$$\beta_{\text{MDF-kin}} = \left(\ln \frac{m_1}{m_2}\right) \Big/ \left(\ln \frac{m_1}{m_3}\right) \tag{6}$$

$$\beta_{\text{MDF-equil}} = \left(\frac{1}{m_1} - \frac{1}{m_2}\right) \Big/ \left(\frac{1}{m_1} - \frac{1}{m_3}\right) \tag{7}$$

where m_x describes the isotopic masses. The difference between the two equations is usually not resolvable in isotope ratios of natural samples, at least with the current analytical precision. A special case are scaling factors related to nuclear volume (eq 8),

DOI: 10.1021/es504683e
Environ. Sci. Technol. 2015, 49, 2606−2624

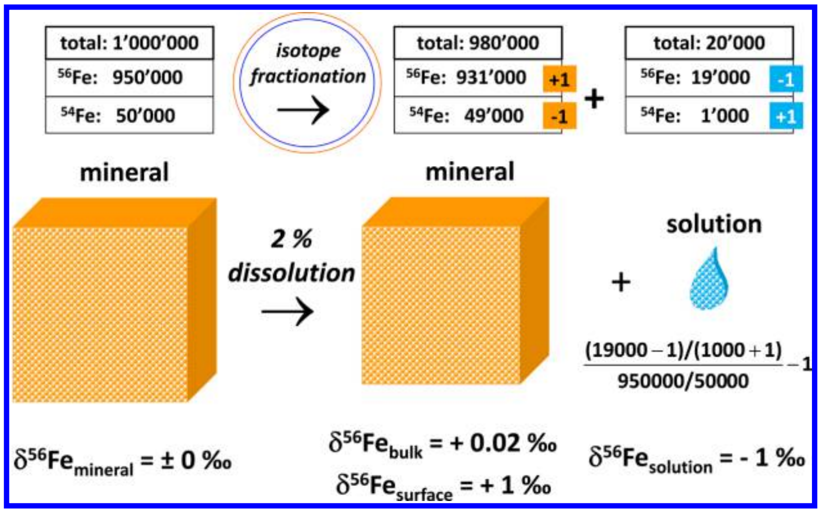

Figure 2. Schematic illustration of metal stable isotope fractionation during mineral dissolution and delta values of the involved metal pools (adapted from Wiederhold[297]). In the presented example, a small fraction (2%) of an iron mineral with 1 million Fe atoms is dissolved (simplified boundary conditions: 95% ^{56}Fe + 5% ^{54}Fe; the surface layer corresponds to 4% of the total mineral). Without isotope fractionation, the dissolved pool would contain 1000 ^{54}Fe atoms. However, metal isotope fractionation manifests itself by the preferential release of one light ^{54}Fe atom resulting in a δ^{56}Fe value of −1 ‰ in solution. The influence on the isotopic signature of the bulk mineral is negligible (+0.02 ‰) due to its larger reservoir size. However, a relative enrichment of heavy isotopes is created at the mineral surface. The general magnitude of metal stable isotope fractionation illustrated in this example is similar to the extent of fractionation observed in nature. However, in order to compare the dimensions, one has to keep in mind that one gram of soil usually contains about 10^{20} Fe atoms.

$$\beta_{\mathrm{NVF}} = \left(\frac{\langle r_1^2 \rangle - \langle r_2^2 \rangle}{\langle r_1^2 \rangle - \langle r_3^2 \rangle} \right) \tag{8}$$

where r_x describes the nuclear charge radii of different isotopes, relevant for very heavy elements (e.g., Hg, Tl, U) exhibiting nuclear volume effects (see section "Nuclear Volume Effect (NVE)"). For most elements, it is sufficient to analyze one isotope ratio (preferably the one which can be measured with highest precision) and other ratios can be inferred using mass-dependent scaling factors. However, this approach is not applicable in the case of mass-independent isotope effects observed for some elements (see section "Mass-Independent Fractionation (MIF)") where the analysis of different isotope ratios yields additional information about samples. Mass-independent isotope effects are expressed as "capital delta" values (Δ) describing deviations of isotope ratios from the mass-dependent trend (often visualized as a line in a three-isotope plot[32] in which two isotope ratios of the same element are plotted against each other) using mass-dependent scaling factors and a reference isotope ratio (eq 9),

$$\Delta^y E = \delta^{y/z}E - (\delta^{x/z}E \times \beta_{\mathrm{MDF}}) \tag{9}$$

where y is the isotope examined for mass-independent fractionation, and x and z are the isotopes describing the mass-dependent trend. This simplified version of the capital delta equation is only valid for δ values smaller than 10‰, otherwise an extended form is required.[33] The same symbol (Δ) is also used in another context as "big delta" describing the difference between two "small delta" values.[32]

■ FRACTIONATION OF STABLE ISOTOPES

Stable isotope fractionation causes a shift in the isotope ratio between reactant and product of a reaction. It is important to realize however that this change is mostly very small, and the isotopic mass balance of the overall system remains unchanged. An isotope enrichment in a certain reservoir must always be balanced by a corresponding depletion in another reservoir. However, it is much easier to induce a significant isotopic change in a small reservoir, whereas the impact of the same process might not be detectable in much larger reservoirs in which the isotope effect is "diluted". Figure 2 presents a schematic example of the magnitude of metal isotope fractionation visualizing an isotope effect of −1‰ in the reaction product and highlighting the importance of reservoir sizes.

Stable isotope fractionation in natural samples can be divided into kinetic and equilibrium effects. Kinetic isotope effects (Figure 3a) are caused by different reaction rates of light and heavy isotopes and are only preserved in incomplete processes. Such processes include, for example, evaporation, diffusion, or biological processes in which the enzymatically mediated breaking of bonds favors those bonds involving light isotopes due to their higher zero-point energies.[34,35] The influence of kinetic effects on the sample isotopic composition depends strongly on the relative extent of reaction progress. The largest effects are observed in remaining reactants which can be strongly enriched in heavy isotopes due to the continuous preferential removal of light isotopes, especially when reactions have proceeded far toward completion. Obviously, if reactants are completely transformed into products, the imprint of kinetic isotope effects during the process is erased and isotope ratios of products are identical to initial reactants. A Rayleigh fractionation model (Figure 4), named after Lord Rayleigh who studied the fractional distillation of mixed liquid, is often used to describe the evolution of isotope ratios during incomplete unidirectional reactions within closed systems. This concept does not only apply to kinetically controlled systems with negligible backward reaction rates, but to all systems in which the product is physically removed or otherwise prevented from isotopically interacting with the reactant. Rayleigh models are very useful to determine fractionation factors for specific processes or to quantify the extent of transformation processes based on isotope data. However, Rayleigh fractionation models

DOI: 10.1021/es504683e
Environ. Sci. Technol. 2015, 49, 2606−2624

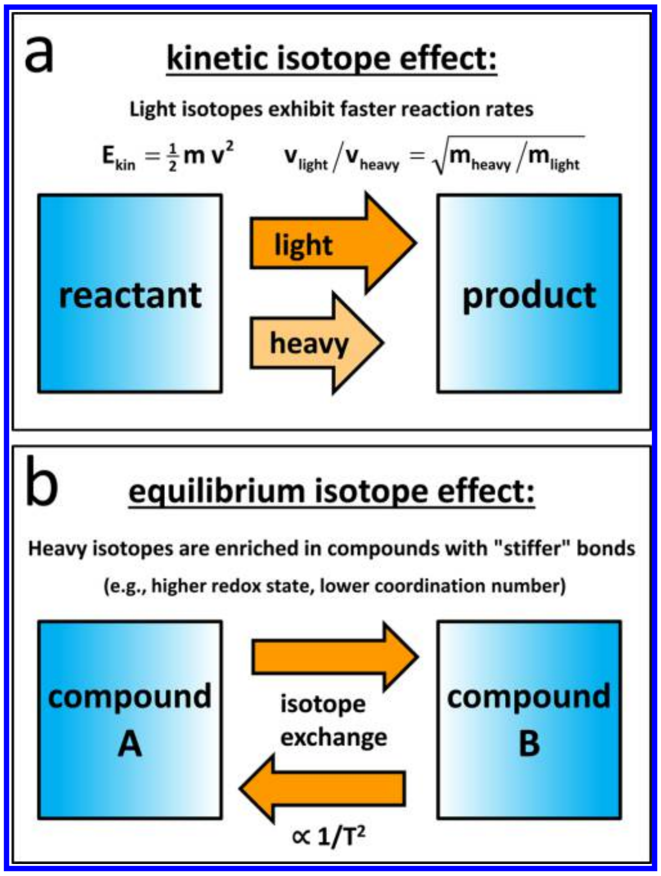

Figure 3. Schematic illustration of kinetic (a) and equilibrium (b) stable isotope fractionation. Natural samples can be affected by both types of fractionation and it is often challenging to elucidate their relative controls on the observed metal stable isotope signatures. Please note that the equations in panel a explaining the "driving force" of kinetic isotope fractionation can usually not be applied directly using m_1 and m_2 as the masses of the studied metal isotopes, because metals are in most cases part of a larger complex or molecule which is reacting in the kinetic process. Furthermore, the indicated trends for equilibrium fractionation in panel b should only be regarded as qualitative rules of thumb (see text for details).

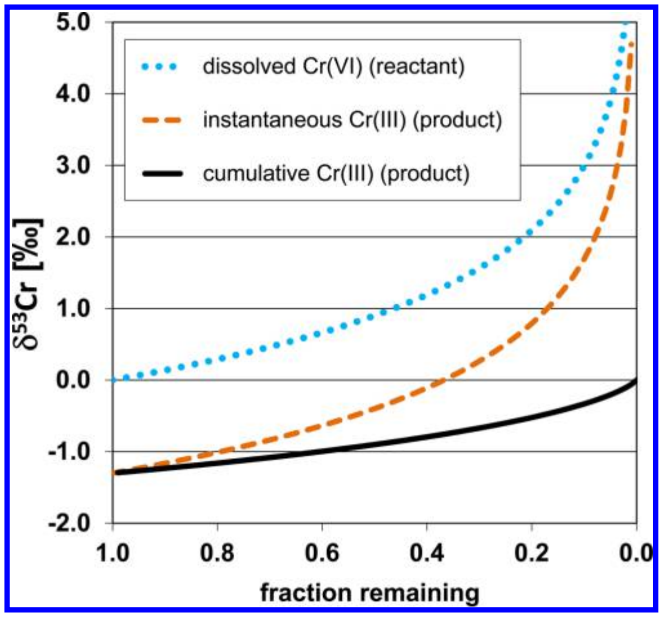

Figure 4. Rayleigh fractionation describing the evolution of isotope ratios in different pools of a unidirectional process, displayed here for the example of Cr isotope ratios (δ^{53}Cr) during the reduction of aqueous Cr(VI) to Cr(III) precipitates, with a starting composition of 0‰ and an enrichment factor ε of −1.3‰. The largest fractionations are found in the reactant (dotted line) at advanced stages of the reaction (low fraction remaining). The difference between the reactant and the instantaneous product (dashed line) corresponds to the enrichment factor ε at all stages of the reaction. In contrast, the difference between the reactant and the cumulative product (solid line) is increasing with progressing reaction and the δ value of the cumulative product of a completed reaction (fraction remaining equals zero) is identical to the starting composition of the reactant. Please see section "Process Tracing" for equations used for calculations of lines.

are only applicable in cases where reactant pools are homogeneous and constantly mixed to allow a continuous preferential removal of light isotopes from the reactant pool.

Equilibrium isotope effects (Figure 3b) occur when two phases react with forward and backward reactions proceeding at equal rates. In this case, the relative isotopic abundance is controlled by energy differences in bonding environments of reaction partners which have reached isotopic equilibrium. However, the time scales required to reach isotopic equilibrium can differ from those required to obtain concentration equilibrium.[7] At isotopic equilibrium heavy isotopes are enriched in "stronger bonding environments", thermodynamically explained by lower zero-point energies of bonds in molecules with heavy isotopes compared to bonds with light isotopes of the same element.[34] Equilibrium isotope effects decrease with increasing temperature (in most cases[35] proportional to $1/T^2$) allowing the application of some isotopic systems as paleothermometer (e.g., oxygen in foraminifera[1]). Molecular modeling can be used to calculate equilibrium isotope effects between elemental species (e.g., complexes and oxidation states).[36] Such computational methods are useful to understand metal isotope fractionation from a theoretical point of view and to predict direction and magnitude of equilibrium isotope effects in specific systems under investigation. Some useful qualitative rules of thumb allow first order predictions as to which of two reaction partners will represent a "stronger bonding environment".[35] First, redox reactions tend to enrich heavy isotopes in oxidized species, causing a corresponding enrichment of light isotopes in reduced species. An example is the equilibrium isotope fractionation between aqueous Fe(III) and Fe(II) with an enrichment of about 3‰ in δ^{56}Fe.[36] Second, metal species with a lower coordination number (e.g., tetrahedral instead of octahedral complexes) and shorter bond length tend to be enriched in heavier isotopes due to their "stronger bonding environment". However, these qualitative rules need to be applied with caution. It is not the strength of the bond per se, but rather its "stiffness" (or more precisely the difference in vibrational frequencies) which determines equilibrium isotope effects.[35] For instance, compounds with thermodynamically very strong Hg−S bonds are enriched in light Hg isotopes (due to pronounced "soft-acid soft-base" interactions and lower vibrational frequencies) relative to compounds with weaker, but tighter Hg−O bonds.[37] In contrast to equilibrium isotope effects which can often be estimated to some extent from theory, kinetic isotope effects depend on many factors (e.g., rates, mechanisms, conditions)[35] and are generally not readily estimated from theoretical calculations.

Mass-Independent Fractionation (MIF). Almost all processes influencing stable isotope ratios in natural samples

DOI: 10.1021/es504683e
Environ. Sci. Technol. 2015, 49, 2606−2624

are mass-dependent, but there are a few notable exceptions where mass-independent fractionation (MIF) has been observed. MIF is defined here as a measured deviation from the mass-dependent fractionation (MDF) trend (eq 9). In contrast to MIF of light elements (e.g., O, S) which often occurs in the gaseous phase due for instance to molecular symmetry or self-shielding processes,[38,39] MIF of heavy elements[40] is usually explained by either nuclear volume effects[41] (in more general terms also referred to as nuclear field shift effects[42,43] encompassing both nuclear size and shape effects) or magnetic isotope effects.[44] Both mechanisms mostly affect odd-mass isotopes and thus MIF of metal isotopes often causes anomalies of odd-mass relative to even-mass isotopes.

Nuclear Volume Effect (NVE). The nuclear volume effect is relevant for very heavy elements (e.g., Hg, Tl, U) and occurs during kinetic and equilibrium reactions. Importantly, only a small part of the NVE is mass-independent in the sense that it creates a deviation from MDF. This is because the nuclear volumes of different isotopes also expand as a nearly linear function of isotopic mass, albeit exhibiting small negative anomalies for some odd-mass isotopes. Due to the similarity of the scaling factors for the NVE (eq 8) vs kinetic or equilibrium MDF (eqs 6 and 7) and the way MIF is quantified (eq 9), only small capital delta values are generated by the NVE, which exhibit an opposite sign to the MDF and increase in magnitude as MDF increases. Compilations of nuclear charge radii for different isotopes are available,[45,46] allowing to assess the potential to cause MIF by the NVE for different stable isotope systems. It is possible to calculate isotope fractionations due to the NVE by relativistic computational methods.[41,37,47−50] For very heavy elements, fractionation by the NVE is generally larger than the "common" fractionation caused by the mass difference. The two effects can go in the same direction (increasing the overall fractionation) or in opposite directions (decreasing the overall fractionation) depending on the elemental species and thus the electron orbitals involved in the chemical reaction. The data available so far suggest that the two effects are of the same sign during the redox transition Tl(I)−Tl(III)[41,49] and of opposite sign during the redox transition U(IV)−U(VI).[42] For Hg, the effects are additive for the redox transition Hg(0)−Hg(II),[41,37] but opposite effects between Hg(II) species have been described as well.[51]

The potential of the NVE to affect natural isotope signatures of other elements is still unclear. Small isotopic anomalies attributed to the NVE were reported from laboratory-scale chemical exchange experiments for many elements (Ti, Cr, Zn, Sr, Mo, Ru, Pd, Cd, Sn, Te, Ba, Nd, Sm, Gd, Yb, Tl, Pb, U).[43,49,52,53] Calculations predict that the influence of the NVE on the overall fractionation is negligible for lighter elements such as S[41] and minor for the transition metals Ni,[54] Cu,[55] and Zn.[56] A somewhat larger influence of the NVE has been calculated for Ru,[41] Cd and Sn,[48] and it may be significant for Pt.[48] In any case, the generated MIF due to the NVE is rather small for all elements (in most cases probably <0.1‰, although somewhat larger effects have been observed in kinetic experiments[57]) and difficult to detect unambiguously in natural environments.[58] However, looking from another angle, the absence of detectable MIF does not exclude an influence of the NVE on the overall extent of isotope fractionation in a sample.

Magnetic Isotope Effect (MIE). The magnetic isotope effect is completely independent of isotopic mass and only affects odd-mass isotopes possessing nuclear spin and magnetic moment. It occurs during kinetically controlled processes linked to radical-pair reactions in which singlet−triplet conversions take place[59] and where reactions rates of isotopes can vary strongly based on presence or absence of nuclear spin and magnetic moment. Depending on the fate of specific radical-pairs in the reaction network, in which some pathways are allowed for certain electron spin states and forbidden for others,[60,61] the reaction products can be strongly enriched or depleted in odd-mass relative to even-mass isotopes. The MIE has been reported in laboratory experiments for many different elements (C, O, Mg, Si, S, Ca, Zn, Ge, Br, Sn, Hg, U) mainly by Buchachenko.[62,63] Since very specific reaction conditions are required for the MIE to be expressed and preserved in the reaction products, its relevance for natural isotope signatures affected by element cycling under environmental conditions is unclear. For instance, the postulated general occurrence of the MIE for Mg during enzymatic phosphorylation, a key process in ATP synthesis, has recently been questioned.[64] So far, an imprint of the MIE in natural samples has only been demonstrated for Hg,[65] where large MIF effects during photochemical processes have been demonstrated experimentally and corresponding signatures detected in environmental samples (e.g., fish, precipitation).[66] Interestingly, photochemical reduction can result in both enrichments (+MIF) or depletions (−MIF) of odd Hg isotopes in the reactants depending on the type of organic ligands present.[67] It remains to be elucidated whether the MIE can influence isotopic distributions of other elements in natural samples too.

MIF Signatures as Additional Tracer. The applicability of MIF signatures as environmental tracer depends on the element studied. Elements with multiple even- and odd-mass isotopes (e.g., Hg, Cd, Sn) permit an independent determination of MDF and MIF signatures by analyzing different isotope ratios in parallel. This enables the use as two-dimensional tracer, as already extensively applied for Hg.[66] On the other hand, MIF of Br, Tl, and U cannot be distinguished from MDF, because only two isotopes are present and no additional information is generated. Figure 5 illustrates the influence of different fractionation mechanisms on Hg isotopes. Here, MIF by the NVE and the MIE can be differentiated by the relative extent of MIF on ^{199}Hg and ^{201}Hg, i.e. the slope in a plot of Δ^{199}Hg vs Δ^{201}Hg (~1.6 for NVE and between 1.0 and 1.36 for MIE).[37,16,66] Not yet considered here is the recent discovery of MIF of even-mass Hg isotopes (Δ^{200}Hg, Δ^{204}Hg) in atmospheric samples[68−70] and in fluorescence lamps,[71] for which the underlying mechanism is still unclear. Elements for which MIF has been detected in natural samples (only O, S, Hg) or observed in laboratory studies are marked in Figure 1.

Extent of Stable Isotope Variation for Chemical Elements. The relative mass difference between stable isotopes, representing the driving force in most fractionating processes, decreases with atomic mass. For instance, while ^{7}Li is about 17% heavier than ^{6}Li, the relative mass difference between ^{26}Mg and ^{24}Mg is 8.3%, between ^{65}Cu and ^{63}Cu 3.2%, and between ^{205}Tl and ^{203}Tl less than 1%. Figure 6a shows the extent of natural stable isotope variation for different elements based on a IUPAC compilation from 2002[72] and a survey of the recent literature. More details are provided in the SI (Table S1) containing descriptions and references for individual elements. The presented values are supposed to illustrate qualitative trends (note logarithmic scale) and the observed ranges for some elements will probably increase in the future. Clearly, the statement found in older textbooks that MDF for elements

DOI: 10.1021/es504683e
Environ. Sci. Technol. 2015, 49, 2606−2624

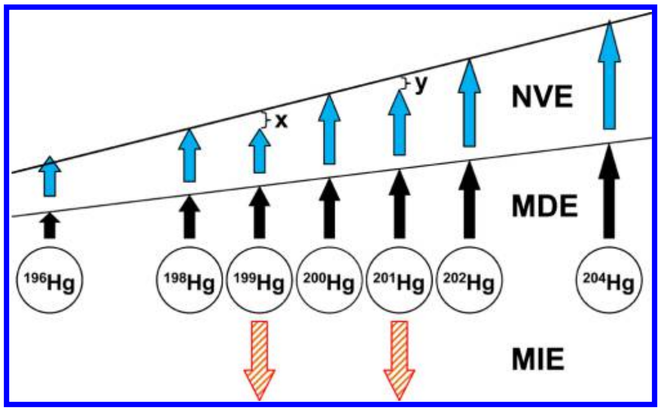

Figure 5. Schematic illustration of fractionation mechanisms for the Hg isotope system (adapted from Wiederhold et al.[37]). The arrows indicate qualitatively the influence of the mass difference effect (MDE), the nuclear volume effect (NVE), and the magnetic isotope effect (MIE) on the seven stable Hg isotopes. Mass-independent fractionation (MIF), which is defined as a measured anomaly compared with the trend of the MDE, is observed mainly for the two odd-mass isotopes ^{199}Hg and ^{201}Hg and can be caused either by the NVE due to their nonlinear increase in nuclear charge radii or the MIE due to their nuclear spin and magnetic moment. The relative extent of the nuclear charge radius anomalies ($x/y = 1.6$) causes the characteristic slope in a $\Delta^{199}Hg/\Delta^{201}Hg$ plot for the NVE in comparison to slopes observed for Hg(II) photoreduction (1.0) and methyl-Hg photodemethylation (~1.36) due to the MIE.[66] The magnitude of MIF due to the NVE is generally much smaller than MIF by the MIE. The MIE occurs only during kinetically controlled processes (in natural systems probably always related to photochemical reactions) whereas the NVE and the MDE occur during both kinetic and equilibrium processes. The relative importance of MDE and NVE on the overall fractionation can vary depending on the reacting species.[37]

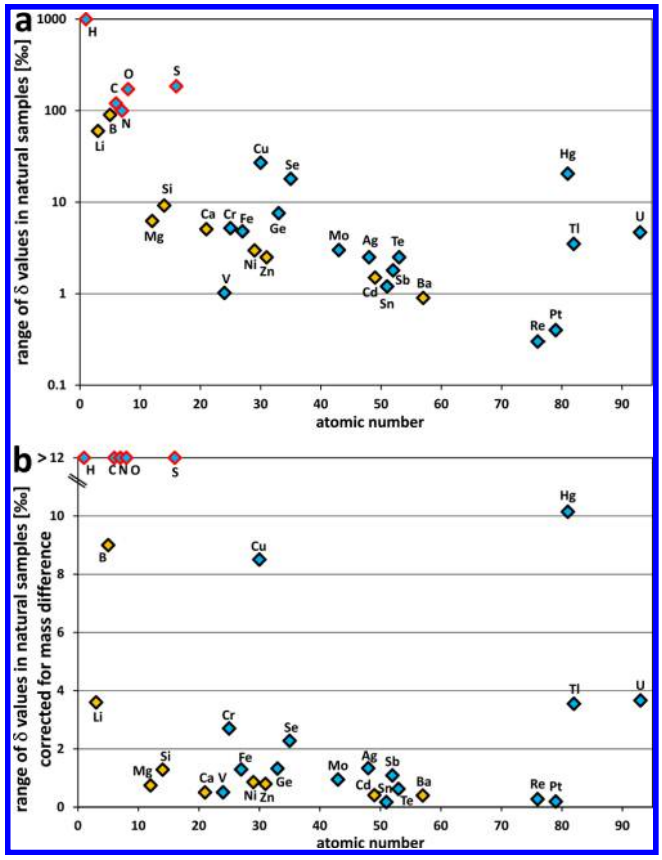

Figure 6. Extent of stable isotope variations of chemical elements plotted against atomic number. Panel a displays the range of δ values observed so far in natural samples on a logarithmic scale. The δ values in panel b were corrected for the relative %-mass difference (divided by $[(mass_{heavy}/mass_{light}) - 1] \times 100$).[74] "Traditional" stable isotopes are marked with a red border and elements usually occurring only in one oxidation state in natural systems are marked with a yellow symbol filling.

heavier than sulfur can be neglected is no longer valid. All elements for which high-precision stable isotope methods have been developed exhibit variations between natural samples of more than 0.1‰, representing the current analytical precision for most elements. There is a generally decreasing trend with increasing atomic mass, but for very heavy elements the NVE (see section "Nuclear Volume Effect (NVE)") becomes important in addition to the fractionation related to mass difference.

In a similar mass range, the extent of natural isotopic variations is linked to the geochemical behavior of the respective elements. This trend is visualized in Figure 6b where isotopic ranges are plotted on a linear scale and corrected for the mass difference effect (inspired by previous figures[73,74]). Elements with multiple oxidation states, variable bonding partners, and presence in different aggregation states exhibit larger isotopic variations than elements always occurring in one oxidation state and bound to the same bonding partners. For instance, silicon is not redox active in nature and always bound to oxygen in tetrahedral coordination. In contrast, sulfur has an active redox chemistry ranging from sulfide (−2) to sulfate (+6), is bound to variable bonding partners (e.g., C, O, metals), and occurs in solid, liquid, and gaseous forms in environmental samples. Therefore, S isotope variations are much larger than those of Si. For transition metals, the redox-active Cu and the redox-inactive Zn (except for anthropogenic samples which may contain elemental Zn) exhibit very different extents of isotopic variation in natural samples. Very large Cu isotope variations were found in porphyry deposits linked to the formation of secondary minerals.[75] The large variations of Cr and Se isotopes can also be explained by redox processes,[76] for Cr partly influenced by anthropogenic pollution.[77] The surprisingly large isotopic range of Hg can be explained by its versatile chemical behavior, active involvement in natural and anthropogenic cycling, and the influence of the NVE. The most extreme Hg isotope variations were found in anthropogenically influenced samples related to ore roasting processes[78] and photochemical processes within fluorescent lamps.[71] Considering the extent to which anthropogenic activities have infiltrated natural element cycles, such anthropogenic metal isotope signatures are probably already affecting the signatures of samples collected in natural ecosystems. In contrast to Hg, the neighboring Pt appears to display much smaller isotopic variations, corresponding to its less diverse geochemical cycle, but maybe also because Pt isotope variations have been barely studied so far.[79] The relatively large variations for Tl and U are again probably related to the influence of the NVE as well as redox processes.

Although it is of course interesting to study elements with large isotopic variations, their application in environmental geochemistry is not necessarily more promising than for those with smaller variations. As discussed in the following sections, the overlapping signals of different fractionating processes represent a major challenge in the deciphering of natural

DOI: 10.1021/es504683e
Environ. Sci. Technol. 2015, 49, 2606−2624

isotope signatures, and therefore elements which are fractionated by a smaller number of processes may ultimately represent more promising tracer systems.

APPLICATION OF METAL STABLE ISOTOPES IN ENVIRONMENTAL GEOCHEMISTRY

Metal isotope signatures can be used in different ways to deduce information about composition and history of environmental samples. The most important applications are source and process tracing.

Source Tracing. Source tracing is based on the mixing of reservoirs with different isotope signatures. If the isotopic compositions of the involved endmembers are known and sufficiently distinct, contributions of different source materials in a sample can be quantified by mixing calculations. Importantly, dilution processes, which can complicate mass balances based on concentration data, do not change stable isotope ratios. The delta value of a sample can be explained by the sum of the delta values of the mixing endmembers multiplied by their relative fractions of the total amount present (eq 10),

$$\delta_{\mathrm{sample}} = \delta_{\mathrm{pool\_A}} \times f_{\mathrm{pool\_A}} + \delta_{\mathrm{pool\_B}} \times f_{\mathrm{pool\_B}} \quad (10)$$

where f describes the relative fraction of the involved pools A and B ($f_{\mathrm{pool\_A}} + f_{\mathrm{pool\_B}} = 1$). Rearranging the equation allows determining the fraction of one endmember (eq 11):

$$f_{\mathrm{pool\_A}} = \frac{\delta_{\mathrm{sample}} - \delta_{\mathrm{pool\_B}}}{\delta_{\mathrm{pool\_A}} - \delta_{\mathrm{pool\_B}}} \quad (11)$$

The principle of mixing two pools is illustrated in Figure 7a−c, visualizing the influence of pool sizes and isotope signatures on the resulting mixture. For example, if the geogenic background in a soil has an isotopic composition of +0.5‰ relative to the reference standard and the soil has been polluted by an anthropogenic source with a delta value of −1.5‰, a delta value of −1.0‰ would indicate an anthropogenic contribution of 75%. Another example for source tracing is the analysis of river water influenced by natural (e.g., rock weathering) and anthropogenic sources (e.g., industrial or urban emissions). A schematic picture of such a system is shown in Figure 7d, inspired by Chen et al.[80] investigating Zn isotopes in the Seine River, France. Source tracing has been applied for several metal stable isotopes and can also include MIF signatures.[81] However, source tracing in natural systems is often complicated because (1) isotopic compositions of mixing endmembers are not known with sufficient precision or not distinct enough, (2) multiple sources contribute to a sample, and (3) the isotope signature of the sample has been additionally affected by fractionating processes. Thus, source tracing works best in systems with well-defined, distinct sources which are not overprinted by fractionating processes.

Process Tracing. Process tracing is based on the concept that a sample has been affected by a transformation process, causing a shift in the isotope signature. An example is the partial transformation of soluble to insoluble elemental species involving a separation of aqueous and solid phases (e.g., reduction of soluble Cr(VI) in groundwater to Cr(III) which precipitates[82]). If the isotopic enrichment factor (ε) for the transformation process is known, the extent of reaction can be quantified from the heavy isotope enrichment in the remaining reactant using a Rayleigh model (Figure 4). Rayleigh model equations can be expressed in different ways, for instance the

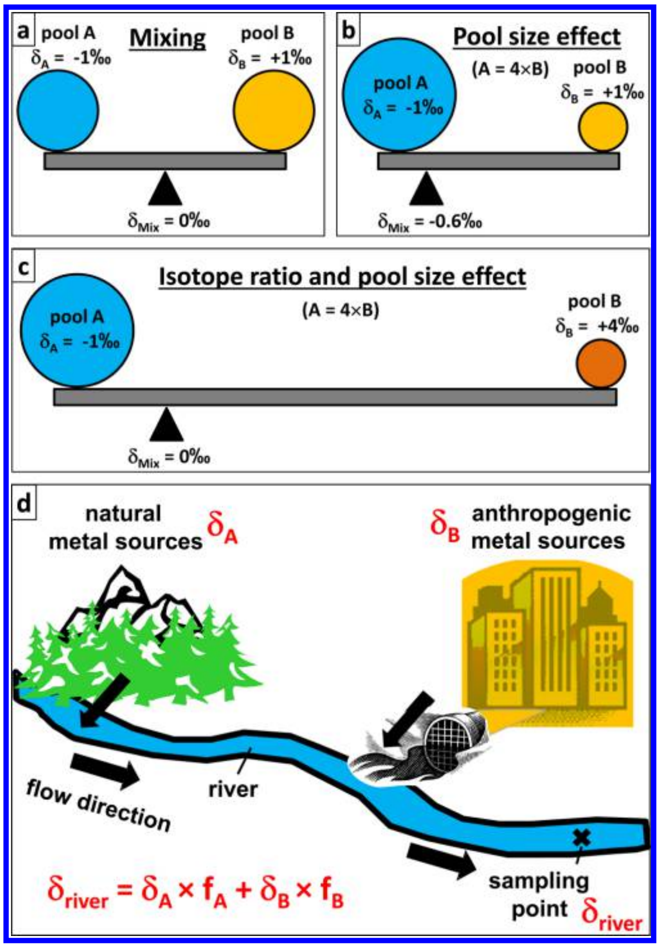

Figure 7. Schematic illustration of the principles of mixing models used for source tracing with metal stable isotope signatures. Panel a depicts the mass balance between two metal pools of opposite isotope signatures and equal size. The effect of different pool sizes (pool A = 4 × pool B) is shown in panel b, and the combined effect of different pool sizes and isotope signatures is illustrated in panel c. Panel d illustrates a schematic example of a natural river system for which the relative fractions of natural and anthropogenic metal sources can be quantified by metal isotope signatures.[80]

reactant delta value (eq 12) is described to a very close approximation by

$$\delta_{\mathrm{reactant}} = \delta_0 + \varepsilon \ln f \quad (12)$$

where δ_0 is the initial reactant composition, ε the isotopic enrichment factor in permil, and f the fraction remaining. The isotopic evolution of the instantaneous product (eq 13) can be calculated as

$$\delta_{\mathrm{inst.product}} = \delta_0 + \varepsilon \ln f + \varepsilon \quad (13)$$

and the cumulative product (eq 14) is described by

$$\delta_{\mathrm{cum.product}} = \delta_0 + \varepsilon \ln f - \frac{\varepsilon \ln f}{1 - f} \quad (14)$$

Again, the power of stable isotope methods for process tracing lies in its independence of dilution effects. For example, decreasing Cr(VI) concentrations in groundwater can be explained by dilution with uncontaminated water or reduction followed by precipitation of Cr(III) phases. Only by analyzing isotope ratios is it possible to demonstrate the occurrence and potentially quantify the extent of reduction.[83] For instance,

DOI: 10.1021/es504683e
Environ. Sci. Technol. 2015, 49, 2606−2624

assuming an enrichment factor of −1.3‰, a water sample which is 2‰ heavier than the source material can be related to a removal of about 80% (Figure 4). Another example for process tracing with metal isotopes is Hg(II) photoreduction in environmental samples[84] resulting in MDF and MIF signatures which can be described with Rayleigh models. A challenge for the quantitative application of process tracing in environmental systems is the variability of isotopic enrichment factors depending on reaction conditions and transport processes. Enrichment factors are often smaller under natural conditions compared with well-mixed laboratory systems.[85] Additionally, several processes with variable isotope effects may occur simultaneously, and mixing with isotopically distinct pools from other sources or partial re-equilibration of product and reactant can complicate the interpretation of natural isotope signatures and the application of simple Rayleigh model approaches.[86] In any case, laboratory studies determining fractionation factors for specific processes are required before signatures of environmental samples can be interpreted for the purpose of process tracing. Despite the progress achieved during the last years, there are still many important fractionation factors unknown. Thus, more experimental work is needed for many elements, before metal isotope signatures can be applied to identify and quantify processes in complex field systems.

■ METAL STABLE ISOTOPE FRACTIONATION DURING INDIVIDUAL PROCESSES

In the following subsections, the current state of knowledge on metal stable isotope fractionation during individual processes is summarized, based on laboratory and theoretical studies or observations from field systems.

Redox Processes. Stable isotope fractionation between different oxidation states of metals represents one of the most important sources of isotopic variability in natural samples. Redox transitions have been used to explain fractionation in various metal isotope systems, but only relatively few studies have determined fractionation factors for specific redox transformations. The equilibrium isotope effect between aqueous Fe(II) and Fe(III) is one of the best studied systems, both from experimental[87] and theoretical[88,36] point of view, exhibiting a large fractionation of about 3‰ in δ^{56}Fe. There are many laboratory or field studies with metals or metalloids in which fractionation during redox processes was observed or inferred, encompassing kinetic and equilibrium effects (e.g., Cr,[89] Cu,[90] Se,[91] Sb,[92] Te,[93] Hg,[94] Tl,[95] U[96]). Theoretical studies provide a fundamental basis for equilibrium isotope fractionation between oxidation states of metals (e.g., Cr,[97] Cu,[98,55] Zn,[99] Se,[100] Hg,[41] Tl[49]), generally predicting an enrichment of heavy isotopes in the oxidized species, except for U,[42] where an inverse redox effect is observed due to the dominance of the NVE (see section "Nuclear Volume Effect (NVE)"). Anthropogenic processing can induce redox changes for metals which usually occur only in one oxidation state in the environment. For example, ore smelting and roasting, the production of elemental metals or engineered nanoparticles for industrial purposes, and combustion processes can cause isotope fractionation due to redox effects (e.g., Zn,[101−104] Cd,[105,106] Hg[107,108,78]) which may be preserved if the process is incomplete and isotopically fractionated metal pools with different oxidation states are released into the environment (e.g., as waste products). Furthermore, electroplating can cause large isotope effects due to redox processes, as experimentally studied for, e.g., Li,[109] Fe,[110] and Zn.[111] Electroplated materials may constitute isotopically distinct metal sources released to the environment as metal wastes and mobilized via corrosion processes. Tracing the imprint of such anthropogenically induced metal isotope signatures in natural environments represents a promising area for future research on heavy metal pollution.[11]

Complexation and Organic Matter Binding. The formation of aqueous solution complexes and the binding of metals to functional groups of organic matter represent another possibility for metal isotope fractionation induced by thermodynamic differences in the respective bonding environments. Even without redox changes, the coordination of ligand complexes can be distinct enough to cause significant metal isotope fractionation. Isotope effects associated with metal binding to organic matter are of special interest in environmental studies and have been examined for several elements, despite the experimental difficulty of separating free and complexed species without inducing fractionation artifacts during the separation procedure. Different experimental designs have been used, such as rapid precipitation of free Fe(III),[112] Donnan-membrane reactors,[113,114] insolubilized humic acid,[115] membrane dialysis bags,[116] and resin beads with functional thiol groups.[37] In most cases, heavy isotope enrichments were observed in organically complexed species compared with free aqueous species and explained by their stronger bonding environments (e.g., Fe,[112,116] Zn,[113] Cu[114,115]). In contrast, organic thiol complexes have been shown to be enriched in light Hg isotopes,[37] consistent with theoretical calculations predicting light Hg isotope enrichments in coordination with reduced sulfur, compared with hydroxyl or chloride ligands in solution. Similarly, organic complexes enriched in light Mg isotopes were explained by a longer bond length compared with corresponding inorganic complexes.[117] Good agreement between experiments and theory was also achieved in studies on Fe(III)−chloro-complexes separated by a liquid extraction method,[118] and B species separated by a reverse osmosis membrane,[119] demonstrating that inorganic complexes can cause significant metal isotope fractionation too. Theoretical studies on the effect of solution speciation and complexation on equilibrium isotope fractionation are available for, e.g., B,[120] Cr,[97] Fe,[121−125] Ni,[54,125] Cu,[55,98,125,126] Zn,[56,99,125,127,128] Ge,[129] Mo,[130] Cd.[131] Clearly, more experimental studies are required to understand the effect of complexation for many metal isotopes. Importantly, if different solution species exhibit different reactivities with respect to other processes (e.g., sorption, precipitation, biological uptake), then fractionation due to solution speciation and complexation can indirectly control isotope effects observed during these processes as well.

Sorption. Sorption refers here to the transfer of dissolved metal species from aqueous to solid phases such as mineral or bacterial surfaces. The environmental fate of metals is often strongly controlled by sorption and determining corresponding fractionation factors is therefore crucial for the interpretation of natural metal isotope signatures. Most experiments have focused on equilibrium isotope effects during sorption by mixing dissolved metal species with a suitable sorbent material and separating supernatant and solid after a certain equilibration time. Analyzing metal isotope ratios in solution and sorbed phase allows determining the fractionation factor associated with sorption. In principle, fractionation factors can be inferred by analyzing only one phase (dissolved or sorbed) and calculating the composition of the other by mass balance. However, this approach can be vulnerable to experimental

DOI: 10.1021/es504683e
Environ. Sci. Technol. 2015, 49, 2606−2624

artifacts, and controlling the concentration and isotopic mass balance of the system by analyzing both components represents the more robust experimental design. Often several batches with a range of fractions sorbed are prepared by changing metal/sorbent ratio or solution pH. In most cases, the magnitude of fractionation is smaller than for redox effects of the same element. For most metals, isotopic enrichment factors of <1‰ were determined for sorption, but larger values were found in some cases (e.g., Mo[132]). Fractionation during sorption is mostly governed by differences in bonding environment between dissolved and sorbed phases[133] or solution species sorbing to a different extent.[51] It is often difficult to verify that equilibrium conditions have been established, and desorption rates are often much slower than adsorption rates, delaying the attainment of isotopic equilibrium. Many studies were conducted with metal oxides (mainly Fe and Mn (oxyhydr)oxides), but other sorbents (e.g., clay minerals, bacteria) were also used. A first summary of metal isotopic enrichment factors during sorption to metal oxides[134] suggested that sorption of cationic species (e.g., Fe, Cu, Zn) causes heavy isotope enrichments in the sorbed phases and sorption of anionic metal species (e.g., Ge,[135] Se,[136] Mo,[132] U[137]) results in light isotope enrichments in the sorbed phases. However, newer studies also reported light isotope enrichments in the sorbed phase for cationic metal species (e.g., Ca,[138] Cu,[139] Cd,[140] Hg[51]). Moreover, depending on experimental conditions and sorbent material, the fractionation was observed to vary in magnitude (e.g., Mo[141]) or even in direction (e.g., B,[142] Zn[143]). For instance, isotope fractionation during metal oxide sorption was recently reported for rare earth elements,[144] with Ce (isotopically light sorbed phase) exhibiting an opposite trend to Nd and Sm (isotopically heavy sorbed phase). In some cases, redox effects can be involved when metal species react with redox-active sorbent surfaces, potentially overprinting the isotope signature of the sorption effect (e.g., Fe,[145,146] Se,[136] Ce,[147] Tl[95,148]). Sorption to bacterial surfaces can be additionally influenced by cell assimilation and organic ligand exudates (e.g., Cu,[149,150] Zn[151,152]). Some studies combine metal isotope analysis with synchrotron-based X-ray absorption data to elucidate the molecular structure of sorbed species (e.g., Cu,[153] Zn,[154,153] Mo,[155,133] Ce,[147] Nd and Sm,[144] Tl,[95] U[137]) helping to identify differences in bonding environments involved in the isotope effect. Theoretical studies predicting equilibrium isotope fractionation between dissolved and sorbed species are available for some elements (e.g., Ge,[156] Mo[133]). Negligible isotope effects were reported for Cr(VI) sorption[157] and U(VI) desorption,[158] relevant for process tracing in polluted aquifers. Importantly, kinetic isotope effects during adsorption[159] and desorption of metals have been studied to a limited extent and require further investigation. For instance, a recent study using enriched Hg isotope tracers revealed slow kinetics and incomplete exchange of Hg(II) with organic complexes and mineral surfaces, suggesting that kinetic isotope effects during the initial sorption step may be partially preserved in the presence of non-exchangeable pools.[160]

Precipitation. The formation of mineral phases can be associated with metal isotope fractionation, but it is often challenging to disentangle kinetic and equilibrium effects.[161] Both light and heavy isotope enrichments in precipitates have been described, depending on system and experimental conditions. Isotope fractionation during precipitation can be described by a Rayleigh model (Figure 4) if the process is unidirectional and no significant re-equilibration of the formed precipitate with the solution phase occurs. In contrast, some studies do not target the fractionation during the precipitation step, but aim to determine the equilibrium fractionation factor between the respective solid phases and dissolved species. Adding an enriched isotope spike allows extrapolating the system evolution in a three-isotope plot toward equilibrium conditions ("three-isotope method"[162]), but is only applicable to elements with at least three isotopes. Kinetic and equilibrium isotope fractionation can also act in opposite directions, that is, isotopically light early precipitates due to kinetic effects, but equilibrium fractionation producing heavy isotope enrichments in solid phases (e.g., FeS[163−165]). A large body of literature exists on carbonate precipitation studying isotope fractionation of e.g., Li,[166,167] Mg,[168−172] Ca,[173−176] Sr,[177] Ba,[178,179] and Fe.[180] Isotope fractionation during precipitation of sulfate minerals has been studied for Ca,[181,182] Mg,[183] Sr,[184] and Ba.[178] Further studies investigated isotope effects during the precipitation of metal (hydr)oxides (e.g., Mg,[117] Fe[185−188]), sulfides (e.g., Fe,[163,164,189,190] Cu,[90] Hg[191]), chlorides (e.g., Ag[192]), amorphous silica,[193,194] and incorporation into silicate structures (e.g., Li,[195] Mg[196]). Theoretical studies on equilibrium metal isotope fractionation for various mineral phases are available for, e.g., Mg,[197,198] Si,[199,200] Ca,[181,198,201] Fe,[202−204,198] Sr,[184] and Hg.[48] However, equilibrium between solid phases is often not attained in low-temperature environments (e.g., sediments, soils) and thus kinetic effects, for instance related to ion desolvation rates[205] prior to precipitation, may be preserved.

Dissolution of Minerals. Dissolution of metals from minerals is important for chemical weathering and nutrient release. Faster dissolution rates of light isotopes at mineral surfaces can cause significant isotope fractionation (Figure 2). Importantly, such a system cannot be described by a Rayleigh model, because in contrast to mineral precipitation from a well-mixed solution pool, only the mineral surface is involved in the dissolution process. Thus, preferential light isotope removal will rapidly form an isotopically heavy surface layer. This layer must first dissolve for the mineral dissolution to continue, limiting the extent of kinetic fractionation. Dissolution proceeds along a moving reaction front and isotope effects are confined to the spatial extent of this layer. However, this reactive surface layer may be large enough to cause measurable isotope effects in solution[206] or even to be preserved over longer time scales in natural systems.[207] In other cases, initial kinetic isotope effects during dissolution have been inferred to be transient and negligible. Isotope effects during the dissolution of polymineralic rocks can also be explained by isotopic heterogeneity between minerals exhibiting different stabilities and therefore involved to a different extent in the dissolution process. Dissolution experiments investigating metal isotope fractionation have been conducted on silicates (e.g., Li,[167] B,[208] Mg,[172,209] Ca,[209] Fe,[210−213] Zn[214]), oxides (e.g., Fe,[186,206,211] Si[215,216]), and other minerals (e.g., Mg,[172] Ca[217]). Isotope effects during metal sulfide dissolution[218−223] were also studied, but for Fe and Cu at least partially overprinted by redox processes. Although simple Rayleigh models are not able to describe metal isotope fractionation during mineral dissolution, other model approaches based on the formation of reactive surface site pools have been developed to describe the evolution of metal isotope ratios in solution with ongoing dissolution.[206,211,213]

Evaporation, Condensation, and Diffusion. Metal isotope fractionation can also be induced by evaporation,

DOI: 10.1021/es504683e
Environ. Sci. Technol. 2015, 49, 2606−2624

condensation, and diffusion.[224] Mercury isotope fractionation during evaporation was described already in 1921.[225,226] Recent experiments[227,228] confirmed that elemental Hg is strongly fractionated isotopically during evaporation and condensation, with large kinetic effects in dynamic systems and smaller effects in equilibrium systems. Except for Hg, evaporation of metals is usually not relevant in the context of environmental geochemistry. However, some metals are volatilized during anthropogenic processing (e.g., combustion, smelting), albeit often combined with redox changes. Experimental data for isotope fractionation during vacuum evaporation are available, for example, for Mg and Si,[229] Ca and Ti,[230] and Cd.[231] Diffusion can induce large kinetic isotope effects and may influence metal isotope signatures of natural samples. Several studies investigated diffusion effects at high temperatures in silicate melts.[232,224] More relevant here are diffusion experiments in water and air reporting isotope fractionation for the metals Fe and Zn,[233] Mo,[234] Hg,[235] and for Cl and Br,[236] and Ar and Ne.[237] Diffusion may also be important for biologically controlled processes.

Biological Cycling. Many metals are involved in biological cycling. In fact, identifying the isotopic imprints of biological activity in environmental samples ("biosignatures") has been a major motivation of metal isotope research from the beginning.[238] However, biological processes are governed by the same physical and chemical principles as abiotic processes. Although many biologically controlled processes can induce significant metal isotope fractionation, the effect is usually linked to one of the processes discussed above (e.g., redox change, complexation, sorption, diffusion). Many biological processes are kinetically controlled (e.g., bond-breaking in enzymatic reactions) and may thus induce kinetic isotope effects. Whether such effects are preserved in signatures of natural samples depends, similarly as for abiotic processes, strongly on pool sizes and the fraction reacted during a transformation process. Equilibrium isotope effects can also be important during biological metal cycling. Many studies have addressed metal isotope fractionation during biologically mediated reduction (e.g., Cl,[239] Fe,[238,240] Cr,[241−243] Se,[244] Te,[93] Hg,[94] U[245]), oxidation (e.g., Fe[246,247]), methylation and demethylation (e.g., Se,[248] Hg[249−251]), and assimilation (e.g., Fe and Mo,[252] Ni,[253] Zn,[254,151] Cu,[149] Cd[255]). Isotope fractionation during uptake and translocation in plants[256,257] has been investigated extensively (e.g., B,[258] Mg,[259,260] Si,[261,262] Cl,[263] Ca,[264,265] Sr,[266] Fe,[267,268] Ni,[269] Cu,[270,271] Zn[272,273]), mostly reporting enrichments of light isotopes in the plant, except for Mg exhibiting isotopically heavy plant biomass. Moreover, metal isotopes in other higher organisms have been studied too (e.g., Ca,[274] Mg,[275] Fe,[276−278] Cu and Zn[279−282]). An extended review of metal isotope fractionation in biological systems is not feasible here, but biological processes clearly play an important role for environmental metal cycling and are also partly responsible for the associated metal isotope fractionation. To decipher complex fractionation patterns of metal isotopes during biological cycling, considering the previous work on traditional stable isotope systems[283,284,3] will certainly be helpful.

■ APPLICATIONS, LIMITATIONS, AND FUTURE PERSPECTIVES

Although the application of metal isotope signatures as tracers in environmental systems is still hampered by missing fractionation factors for many processes, the scientific field has made impressive progress over the last years. Important parameters and governing principles controlling metal isotope fractionation have been elucidated for many elements by a combination of experimental, theoretical, and field-based studies, complementing each other toward a comprehensive picture of metal isotope geochemistry. Integrating the results of all three approaches will enable the environmental geochemistry community to further develop the novel tool of metal isotope analysis to address important scientific questions. Nonetheless, the application of metal isotope signatures as tracers will remain challenging, especially in complex systems influenced by multiple processes and metal sources. In many cases, metal isotope approaches will be most powerful in systems which have already been characterized using other methods (e.g., concentration, speciation) and where the analysis of metal isotope ratios on selected samples allows testing previously defined hypotheses. As general advice, especially for newcomers interested in entering the field of metal isotope research, I suggest bearing in mind the following principles:

(1) Spend enough time on method development to verify the accuracy and precision of your analytical method, not only for standard materials but also the sample matrix you are interested in.
(2) Consider the mass balance of your system to understand how metal isotope fractionation can potentially affect different pools, and plan the sampling approach accordingly.
(3) Collect as many analytical parameters as possible in addition to metal isotope ratios which will greatly help in the interpretation of your isotope data.
(4) Pay close attention to the relative importance of kinetic and equilibrium conditions in your investigated system because they may exert an important influence on your observed signatures.
(5) Combine metal isotope signatures with additional tools (e.g., spectroscopic techniques, extractions, modeling) to understand the speciation and fate of the studied metal in your samples.

Considering the difficulty of interpreting isotope signatures of individual elements in complex environments, the combination of isotopic systems may prove useful in the characterization of field samples. For instance, source tracing in a two-dimensional space potentially allows distinguishing samples which have overlapping isotope signatures in one element. Multidimensional isotope tracing possibilities are already embedded in those isotope systems exhibiting MDF and MIF expressed in different ratios (Hg) and those affected by radiogenic processes and stable isotope fractionation in parallel (e.g., Sr,[266] Ca[285]). In other cases, combining metal isotope signatures of different elements may yield similar multidimensional results. Another promising approach for the study of soils and sediments represents the combination of sequential extraction and size fractionation methods with metal isotope analysis to gain insight into isotopic differences between various metal pools present in natural samples. Such methods have already been successfully applied for several elements (e.g., Ca,[286] Fe,[287,207] Cu,[288,289] Zn,[288] Se,[290] Hg[291,292]), but a careful method selection is required and standard procedures may need to be adapted to avoid fractionation artifacts.[293] For some elements, the determination of species-specific isotope signatures represents another

DOI: 10.1021/es504683e
Environ. Sci. Technol. 2015, 49, 2606−2624

promising research area by coupling a chromatograph system to MC-ICP-MS.[294] Analytical advances will further increase the sensitivity of existing metal isotope methods, facilitating the study of natural systems with low metal concentrations currently requiring extensive pre-enrichment steps prior to analysis (e.g., dilute waters, atmospheric samples). Additionally, new model approaches are being developed to describe metal isotope fractionation in complex natural systems.[295,296] Research on metal stable isotopes is clearly moving at a fast pace and developing on many fronts in parallel. Future work will identify the most useful tracer systems for specific applications in environmental geochemistry. Our understanding is still incomplete and a multitude of questions remain open, but one should keep in mind that compared to the traditional stable isotope systems which have evolved over more than half a century, research on metal stable isotope signatures is still in its beginning.

■ ASSOCIATED CONTENT

Ⓢ Supporting Information

The Supporting Information contains short descriptions of analytical techniques for metal stable isotopes and a table on individual elements with references to reviews, method papers, and selected studies. This material is available free of charge via the Internet at http://pubs.acs.org.

■ AUTHOR INFORMATION

Corresponding Author

*Phone: +41-44-6336008; fax: +41-44-6331118; e-mail: wiederhold@env.ethz.ch; jan.wiederhold@gmx.net.

Notes

The authors declare no competing financial interest.

■ ACKNOWLEDGMENTS

I thank Martin Jiskra, Robin Smith, Thomas Borch, Daniel Obrist, Iso Christl, Michael Köbberich, Thomas D. Bullen, and four anonymous reviewers for helpful comments, Ruben Kretzschmar, Bernard Bourdon, Maria Schönbächler, and Derek Vance for financial support, and the participants of the EnvironMetal Isotopes 2013 conference for inspiring discussions.

■ REFERENCES

(1) Hoefs, J. *Stable Isotope Geochemistry*; Springer: Berlin, 2009.
(2) Fry, B. *Stable Isotope Ecology*; Springer: New York, 2006.
(3) *Stable Isotopes in Ecology and Environmental Science*; Michener, R., Lajtha, K., Eds.; Blackwell: Oxford, 2007.
(4) *Handbook of Stable Isotope Analytical Techniques*; de Groot, P. A., Ed.; Elsevier: Amsterdam, 2008.
(5) Young, E. D.; Manning, C. E.; Schauble, E. A.; Shahar, A.; Macris, C. A.; Lazar, C.; Jordan, M. High-temperature equilibrium isotope fractionation of non-traditional stable isotopes: Experiments, theory, and applications. *Chem. Geol.* **2015**, *395*, 176−195.
(6) Wasylenki, L. E. Establishing the basis for using stable isotope ratios of metals as paleoredox proxies. In *Isotopic Analysis*, Chapter 11; Vanhaecke, F., Degryse, P.; Eds.; Wiley-VCH: Weinheim, 2012; pp 317−350.
(7) Johnson, C. M.; Beard, B. L.; Albarède, F.; Eds. *Geochemistry of non-traditional stable isotopes*, Reviews in Mineralogy and Geochemistry 55; Mineralogical Society of America and Geochemical Society: Washington, DC, 2004.
(8) Weiss, D. J.; Rehkämper, M.; Schoenberg, R.; McLaughlin, M.; Kirby, J.; Campbell, P. G. C.; Arnold, T.; Chapman, J.; Peel, K.; Gioia, S. Application of nontraditional stable-isotope systems to the study of sources and fate of metals in the environment. *Environ. Sci. Technol.* **2008**, *42*, 655−664.
(9) Bullen, T. D.; Eisenhauer, A. Metal stable isotopes signals in the environment. *Elements* **2009**, *5*, 6.
(10) Baskaran, M. *Handbook of Environmental Isotope Geochemistry*; Springer: Heidelberg, 2012.
(11) Bullen, T. D. Stable isotopes of transition and post-transition metals as tracers in environmental studies. In *Handbook of Environmental Isotope Geochemistry*, Chapter 10; Baskaran, M., Ed.; Springer: Heidelberg, 2012; pp 177−203.
(12) Bullen, T. D. Metal stable isotopes in weathering and hydrology. In *Treatise on Geochemistry*, 2nd ed.; Elsevier: New York, 2014; Vol. *7.10*, pp 329−359.
(13) Romanek, C. S.; Beard, B.; Anbar, A. D.; Andrus, C. F. T. Nontraditional stable isotopes in environmental sciences. In *Environmental Isotopes in Biodegradation and Bioremediation*, Chapter 12; Aelion, C. M., Höhener, P., Hunkeler, D., Aravena, R., Eds.; CRC Press: Boca Raton, 2010; pp 385−435.
(14) Kyser, K. Isotopes as tracers of elements across the geosphere−biosphere interface. In *Isotopic Analysis*, Chapter 12; Vanhaecke, F., Degryse, P.; Eds.; Wiley-VCH: Weinheim, 2012; pp 351−372.
(15) Tanimizu, M.; Sohrin, Y.; Hirata, T. Heavy element stable isotope ratios: Analytical approaches and applications. *Anal. Bioanal. Chem.* **2013**, *405*, 2771−2783.
(16) Eiler, J. M.; Bergquist, B.; Bourg, I.; Cartigny, P.; Farquhar, J.; Gagnon, A.; Guo, W.; Halevy, I.; Hofmann, A.; Larson, T. E.; Levin, N.; Schauble, E. A.; Stolper, D. Frontiers of stable isotope geoscience. *Chem. Geol.* **2014**, *372*, 119−143.
(17) Heger, A.; Fröhlich, C.; Truran, J. W. Origin of the elements. In *Treatise on Geochemistry*, 2nd ed.; Elsevier: New York, 2014; Vol. *2.1*, pp 1−14.
(18) Blum, J. D.; Erel, Y. Radiogenic isotopes in weathering and hydrology. In *Treatise on Geochemistry*; Elsevier: New York, 2003; Vol. *5.12*, pp 365−392.
(19) Capo, R. C.; Stewart, B. W.; Chadwick, O. A. Strontium isotopes as tracers of ecosystem processes: Theory and methods. *Geoderma* **1998**, *82*, 197−225.
(20) Shand, P.; Darbyshire, D. P. F.; Love, A. J.; Edmunds, W. M. Sr isotopes in natural waters: Applications to source characterization and water-rock interaction in contrasting landscapes. *Appl. Geochem.* **2009**, *24*, 574−586.
(21) Slovak, N. M.; Paytan, A. Applications of Sr isotopes in archaeology. In *Handbook of Environmental Isotope Geochemistry*, Chapter 35; Baskaran, M., Ed.; Springer: Heidelberg, 2012; pp 743−768.
(22) Le Roux, G.; Sonke, J. E.; Cloquet, C.; Aubert, D.; de Vleeschouwer, F. Comment on "The biosphere: A homogeniser of Pb-isotope signals" by C. Reimann, B. Flem, A. Arnoldussen, P. Englmaier, T.E. Finne, F. Koller and Ø. Nordgulen. *Appl. Geochem.* **2008**, *23*, 2789−2792.
(23) Komarek, M.; Ettler, V.; Chrastny, V.; Mihaljevič, M. Lead isotopes in environmental sciences: A review. *Environ. Int.* **2008**, *34*, 562−577.
(24) von Blanckenburg, F.; Willenbring, J. K. Cosmogenic nuclides: Dates and rates of Earth-surface change. *Elements* **2014**, *10*, 341−346.
(25) Mabit, L.; Benmansour, M.; Abril, J. M.; Walling, D. E.; Meusburger, K.; Iurian, A. R.; Bernard, C.; Tarján, S.; Owens, P. N.; Blake, W. H.; Alewell, C. Fallout 210Pb as a soil and sediment tracer in catchment sediment budget investigations: A review. *Earth Sci. Rev.* **2014**, *138*, 335−351.
(26) Stürup, S.; Hansen, H. R.; Gammelgaard, B. Application of enriched stable isotopes as tracers in biological systems: A critical review. *Anal. Bioanal. Chem.* **2008**, *390*, 541−554.
(27) Croteau, M.-N.; Cain, D. J.; Fuller, C. C. Novel and nontraditional use of stable isotope tracers to study metal bioavailability from natural particles. *Environ. Sci. Technol.* **2013**, *47*, 3424−3431.

DOI: 10.1021/es504683e
Environ. Sci. Technol. 2015, 49, 2606−2624

(28) Hamon, R. E.; Parker, D. R.; Lombi, E. Advances in isotopic dilution techniques in trace element research: A review of methodologies, benefits, and limitations. *Adv. Agron.* **2008**, *99*, 289−343.

(29) Björn, E.; Larsson, T.; Lambertsson, L.; Skyllberg, U.; Frech, W. Recent advances in mercury speciation analysis with focus on spectrometric methods and enriched stable isotope applications. *Ambio* **2007**, *36*, 443−451.

(30) Coplen, T. B. Guidelines and recommended terms for expression of stable-isotope-ratio and gas-ratio measurement results. *Rapid Commun. Mass Spectrom.* **2011**, *25*, 2538−2560.

(31) Young, E. D.; Galy, A.; Nagahara, H. Kinetic and equilibrium mass-dependent isotope fractionation laws in nature and their geochemical and cosmochemical significance. *Geochim. Cosmochim. Acta* **2002**, *66*, 1095−1104.

(32) Criss, B. E.; Farquhar, J. Abundance, notation, and fractionation of light stable isotopes. *Rev. Mineral. Geochem.* **2008**, *68*, 15−30.

(33) Blum, J. D.; Bergquist, B. A. Reporting of variations in the natural isotopic composition of mercury. *Anal. Bioanal. Chem.* **2007**, *388*, 353−359.

(34) Criss, B. E. *Principles of Stable Isotope Distribution*; Oxford University Press: New York, 1999.

(35) Schauble, E. Applying stable isotope fractionation theory to new systems. *Rev. Mineral. Geochem.* **2004**, *55*, 65−112.

(36) Schauble, E. A.; Méheut, M.; Hill, P. S. Combining metal stable isotope fractionation theory with experiments. *Elements* **2009**, *5*, 369−374.

(37) Wiederhold, J. G.; Cramer, C. J.; Daniel, K.; Infante, I.; Bourdon, B.; Kretzschmar, R. Equilibrium mercury isotope fractionation between dissolved Hg(II) species and thiol-bound Hg. *Environ. Sci. Technol.* **2010**, *44*, 4191−4197.

(38) Thiemens, M. H.; Chakraborty, S.; Dominguez, G. The physical chemistry of mass-independent isotope effects and their observation in nature. *Annu. Rev. Phys. Chem.* **2012**, *63*, 155−177.

(39) Thiemens, M. H. Introduction to chemistry and applications in nature of mass independent isotope effects special feature. *Proc. Natl. Acad. Sci. U.S.A.* **2013**, *110*, 17631−17637.

(40) Epov, V. N.; Malinovskiy, D.; Vanhaecke, F.; Bégué, D.; Donard, O. F. X. Modern mass spectrometry for studying mass-independent fractionation of heavy stable isotopes in environmental and biological sciences. *J. Anal. At. Spectrom.* **2011**, *26*, 1142−1156.

(41) Schauble, E. A. Role of nuclear volume in driving equilibrium stable isotope fractionation of mercury, thallium, and other very heavy elements. *Geochim. Cosmochim. Acta* **2007**, *71*, 2170−2189.

(42) Bigeleisen, J. Nuclear size and shape effects in chemical reactions. Isotope chemistry of the heavy elements. *J. Am. Chem. Soc.* **1996**, *118*, 3676−3680.

(43) Fujii, T.; Moynier, F.; Albarède, F. The nuclear field shift effect in chemical exchange reactions. *Chem. Geol.* **2009**, *267*, 139−156.

(44) Buchachenko, A. L. MIE versus CIE - comparative analysis of magnetic and classical isotope effects. *Chem. Rev.* **1995**, *95*, 2507−2528.

(45) Fricke, G.; Heilig, K. *Nuclear Charge Radii* (Landolt-Börnstein: Numerical Data and Functional Relationships in Science and Technology New Series: Group I: Elementary Particles, Nuclei and Atoms); Springer: Berlin, 2004; Vol. *20*.

(46) Angeli, I.; Gangrsky, Y. P.; Marinova, K. P.; Boboshin, I. N.; Komarov, S. Y.; Ishkhanov, B. S.; Varlamov, V. V. N and Z dependence of nuclear charge radii. *J. Phys. G* **2009**, *36* (085102), 26pp.

(47) Abe, M.; Suzuki, T.; Fujii, Y.; Hada, M.; Hirao, K. Ligand effect on uranium isotope fractionations caused by nuclear effects: An ab initio relativistic molecular orbital study. *J. Chem. Phys.* **2010**, *133*, 044309.

(48) Schauble, E. A. Modeling nuclear volume isotope effects in crystals. *Proc. Natl. Acad. Sci. U.S.A.* **2013**, *110*, 17714−17719.

(49) Fujii, T.; Moynier, F.; Agranier, A.; Ponzevera, E.; Abe, M.; Uehara, A.; Yamana, H. Nuclear field shift effect in isotope fractionation of thallium. *J. Radioanal. Nucl. Chem.* **2013**, *296*, 261−265.

(50) Abe, M.; Hada, M.; Suzuki, T.; Fujii, Y.; Hirao, K. Theoretical study of isotope enrichment caused by nuclear volume effect. *J. Comput. Chem. Jpn.* **2014**, *13*, 92−104.

(51) Jiskra, M.; Wiederhold, J. G.; Bourdon, B.; Kretzschmar, R. Solution speciation controls mercury isotope fractionation of Hg(II) sorption to goethite. *Environ. Sci. Technol.* **2012**, *46*, 6654−6662.

(52) Fujii, T.; Moynier, F.; Agranier, A.; Ponzevera, E.; Abe, M. Isotope fractionation of palladium in chemical exchange reaction. *Proc. Radiochim. Acta* **2011**, *1*, 339−344.

(53) Fujii, T.; Moynier, F.; Agranier, A.; Ponzevera, E.; Abe, M. Nuclear field shift effect of lead in ligand exchange reaction using a crown ether. *Proc. Radiochim. Acta* **2011**, *1*, 387−392.

(54) Fujii, T.; Moynier, F.; Dauphas, N.; Abe, M. Theoretical and experimental investigation of nickel isotopic fractionation in species relevant to modern and ancient oceans. *Geochim. Cosmochim. Acta* **2011**, *75*, 469−482.

(55) Fujii, T.; Moynier, F.; Abe, M.; Nemoto, K.; Albarède, F. Copper isotope fractionation between aqueous compounds relevant to low temperature geochemistry and biology. *Geochim. Cosmochim. Acta* **2013**, *110*, 29−44.

(56) Fujii, T.; Moynier, F.; Telouk, P.; Abe, M. Experimental and theoretical investigation of isotope fractionation of zinc between aqua, chloro, and macrocyclic complexes. *J. Phys. Chem. A* **2010**, *114*, 2543−2552.

(57) Zheng, W.; Hintelmann, H. Nuclear field shift effect in isotope fractionation of mercury during abiotic reduction in the absence of light. *J. Phys. Chem. A* **2010**, *114*, 4238−4245.

(58) Moynier, F.; Fujii, T.; Brennecka, G. A.; Nielsen, S. G. Nuclear field shift in natural environments. *C. R. Geoscience* **2013**, *345*, 150−159.

(59) Turro, N. J. Influence of nuclear spin on chemical reactions: Magnetic isotope and magnetic field effects (a review). *Proc. Natl. Acad. Sci. U.S.A.* **1983**, *80*, 609−621.

(60) Epov, V. N. Magnetic isotope effect and theory of atomic orbital hybridization to predict a mechanism of chemical exchange reactions. *Phys. Chem. Chem. Phys.* **2011**, *13*, 13222−13231.

(61) Salikhov, K. M. *Magnetic Isotopes Effect in Radical Reactions: An Introduction*. Springer, Wien, 1996.

(62) Buchachenko, A. L. *Magnetic Isotope Effect in Chemistry and Biochemistry*; Nova Science Publishers, New York, 2009.

(63) Buchachenko, A. L. Mass-independent isotope effects. *J. Phys. Chem. B* **2013**, *117*, 2231−2238.

(64) Crotty, D.; Silkstone, G.; Poddar, S.; Ranson, R.; Prina-Mello, A.; Wilson, M. T.; Coey, J. M. D. Reexamination of magnetic isotope and field effects on adenosine triphosphate production by creatine kinase. *Proc. Natl. Acad. Sci. U.S.A.* **2012**, *109*, 1437−1442.

(65) Bergquist, B. A.; Blum, J. D. Mass-dependent and -independent fractionation of Hg isotopes by photoreduction in aquatic systems. *Science* **2007**, *318*, 417−420.

(66) Blum, J. D.; Sherman, L. S.; Johnson, M. W. Mercury isotopes in earth and environmental sciences. *Annu. Rev. Earth Planet. Sci.* **2014**, *42*, 249−269.

(67) Zheng, W.; Hintelmann, H. Isotope fractionation of mercury during its photochemical reduction by low-molecular-weight organic compounds. *J. Phys. Chem. A* **2010**, *114*, 4246−4253.

(68) Gratz, L. E.; Keeler, G. J.; Blum, J. D.; Sherman, L. S. Isotopic composition and fractionation of mercury in Great Lakes precipitation and ambient air. *Environ. Sci. Technol.* **2010**, *44*, 7764−7770.

(69) Chen, J.; Hintelmann, H.; Feng, X.; Dimock, B. Unusual fractionation of both odd and even mercury isotopes in precipitation from Peterborough, ON, Canada. *Geochim. Cosmochim. Acta* **2012**, *90*, 33−46.

(70) Demers, J. D.; Blum, J. D.; Zak, D. R. Mercury isotopes in a forested ecosystem: Implications for air-surface exchange dynamics and the global mercury cycle. *Global Biogeochem. Cycles* **2013**, *27*, 222−238.

(71) Mead, C.; Lyons, J.; Johnson, T.; Anbar, A. Unique Hg stable isotope signatures of compact fluorescent lamp-sourced Hg. *Environ. Sci. Technol.* **2013**, *47*, 2542−2547.

DOI: 10.1021/es504683e
Environ. Sci. Technol. 2015, 49, 2606−2624

(72) Coplen, T. B.; Böhlke, J. K.; De Bièvre, P.; Ding, T.; Holden, N. E.; Hopple, J. A.; Krouse, H. R.; Lamberty, A.; Peiser, H. S.; Révész, K. M.; Rieder, S. E.; Rosman, K. J. R.; Roth, E.; Taylor, P. D. P.; Vocke, R. D., Jr; Xiao, Y. K. Isotopic abundance variations of selected elements. *Pure Appl. Chem.* **2002**, *74*, 1987−2017.

(73) Smith, C. N.; Kesler, S. E.; Klaue, B.; Blum, J. D. Mercury isotope fractionation in fossil hydrothermal systems. *Geology* **2005**, *33*, 825−828.

(74) Johnston, D. T.; Fischer, W. W. Stable isotope geology. In *Fundamentals of Geobiology*, Chapter 14; Knoll, A. H., Canfield, D. E., Konhauser., K. O.; Eds.; Blackwell: Chichester, 2012; pp 250−268.

(75) Mathur, R.; Titley, S.; Barra, F.; Brantley, S.; Wilson, M.; Phillips, A.; Munizaga, F.; Makseav, V.; Vervoort, J.; Hart, G. Exploration potential of Cu isotope fractionation in porphyry copper deposits. *J. Geochem. Explor.* **2009**, *102*, 1−6.

(76) Johnson, T. M. Stable isotopes of Cr and Se as tracers of redox processes in Earth surface environments. In *Handbook of Environmental Isotope Geochemistry*, Chapter 9; Baskaran, M., Ed.; Springer: Heidelberg, 2012; pp 155−175.

(77) Novak, M.; Chrastny, V.; Cadkova, E.; Farkas, J.; Bullen, T. D.; Tylcer, J.; Szurmanova, Z.; Cron, M.; Prechova, E.; Curik, J.; Stepanova, M.; Pasava, J.; Erbanova, L.; Houskova, M.; Puncochar, K.; Hellerich, L. A. Common occurrence of a positive δ^{53}Cr shift in Central European waters contaminated by geogenic/industrial chromium relative to source values. *Environ. Sci. Technol.* **2014**, *48*, 6089−6096.

(78) Smith, R. S.; Wiederhold, J. G.; Jew, A. D.; Brown, G. E., Jr.; Bourdon, B.; Kretzschmar, R. Small-scale studies of roasted ore waste reveal extreme ranges of stable mercury isotope signatures. *Geochim. Cosmochim. Acta* **2014**, *137*, 1−17.

(79) Creech, J. B.; Baker, J. A.; Handler, M. R.; Bizzarro, M. Platinum stable isotope analysis of geological standard reference materials by double-spike MC-ICPMS. *Chem. Geol.* **2014**, *363*, 293−300.

(80) Chen, J. B.; Gaillardet, J.; Louvat, P. Zinc isotopes in the Seine River waters, France: A probe of anthropogenic contamination. *Environ. Sci. Technol.* **2008**, *42*, 6494−6501.

(81) Estrade, N.; Carignan, J.; Donard, O. F. X. Isotope tracing of atmospheric mercury sources in an urban area of northeastern France. *Environ. Sci. Technol.* **2010**, *44*, 6062−6067.

(82) Ellis, A. S.; Johnson, T. M.; Bullen, T. D. Chromium isotopes and the fate of hexavalent chromium in the environment. *Science* **2002**, *295*, 2060−2062.

(83) Berna, E. C.; Johnson, T. M.; Makdisi, R. S.; Basu, A. Cr stable isotopes as indicators of Cr(VI) reduction in groundwater: A detailed time-series study of a point-source plume. *Environ. Sci. Technol.* **2010**, *44*, 1043−1048.

(84) Sherman, L. S.; Blum, J. D.; Johnson, K. P.; Keeler, G. J.; Barres, J. A.; Douglas, T. A. Mass-independent fractionation of mercury isotopes in arctic snow driven by sunlight. *Nat. Geosc.* **2010**, *3*, 173−177.

(85) Clark, S. K.; Johnson, T. M. Effective isotopic fractionation factors for solute removal by reactive sediments: A laboratory microcosm and slurry study. *Environ. Sci. Technol.* **2008**, *42*, 7850−7855.

(86) Lutz, S. R.; Van Breukelen, B. M. Combined source apportionment and degradation quantification of organic pollutants with CSIA: 1. Model derivation. *Environ. Sci. Technol.* **2014**, *48*, 6220−6228.

(87) Welch, S. A.; Beard, B. L.; Johnson, C. M.; Braterman, P. S. Kinetic and equilibrium Fe isotope fractionation between aqueous Fe(II) and Fe(III). *Geochim. Cosmochim. Acta* **2003**, *67*, 4231−4250.

(88) Anbar, A. D.; Jarzecki, A. A.; Spiro, T. G. Theoretical investigation of iron isotope fractionation between $Fe(H_2O)_6^{3+}$ and $Fe(H_2O)_6^{2+}$: Implications for iron stable isotope geochemistry. *Geochim. Cosmochim. Acta* **2005**, *69*, 825−837.

(89) Wang, X.; Johnson, T. M.; Ellis, A. S. Equilibrium isotopic fractionation and isotopic exchange kinetics between Cr(III) and Cr(VI). *Geochim. Cosmochim. Acta* **2015**, *153*, 72−90.

(90) Ehrlich, S.; Butler, I.; Halicz, L.; Rickard, D.; Oldroyd, A.; Matthews, A. Experimental study of the copper isotope fractionation between aqueous Cu(II) and covellite, CuS. *Chem. Geol.* **2004**, *209*, 259−269.

(91) Ellis, A. S.; Johnson, T. M.; Bullen, T. D.; Herbel, M. J. Stable isotope fractionation of selenium by natural microbial consortia. *Chem. Geol.* **2003**, *195*, 119−129.

(92) Rouxel, O.; Ludden, J.; Fouquet, Y. Antimony isotope variations in natural systems and implications for their use as geochemical tracers. *Chem. Geol.* **2003**, *200*, 25−40.

(93) Baesman, S. M.; Bullen, T. D.; Dewald, J.; Zhang, D.; Curran, S.; Islam, F. S.; Beveridge, T. J.; Oremland, R. S. Formation of tellurium nanocrystals during anaerobic growth of bacteria that use Te oxyanions as respiratory electron acceptors. *Appl. Environ. Microbiol.* **2007**, *73*, 2135−2143.

(94) Kritee, K.; Blum, J. D.; Johnson, M. W.; Bergquist, B.; Barkay, T. Mercury stable isotope fractionation during reduction of Hg(II) to Hg(0) by mercury resistant bacteria. *Environ. Sci. Technol.* **2007**, *41*, 1889−1895.

(95) Peacock, C. L.; Moon, E. M. Oxidative scavenging of thallium by birnessite: Controls on thallium sorption and stable isotope fractionation in marine ferromanganese precipitates. *Geochim. Cosmochim. Acta* **2012**, *84*, 297−313.

(96) Wang, X.; Johnson, T. M.; Lundstrom, C. C. Isotope fractionation during oxidation of tetravalent uranium by dissolved oxygen. *Geochim. Cosmochim. Acta* **2015**, *150*, 160−170.

(97) Schauble, E.; Rossman, G. R.; Taylor, H. P. Theoretical estimates of equilibrium chromium-isotope fractionations. *Chem. Geol.* **2004**, *205*, 99−114.

(98) Sherman, D. M. Equilibrium isotopic fractionation of copper during oxidation/reduction, aqueous complexation and ore-forming processes: Predictions from hybrid density functional theory. *Geochim. Cosmochim. Acta* **2013**, *118*, 85−97.

(99) Black, J. R.; Kavner, A.; Schauble, E. A. Calculation of equilibrium stable isotope partition functions for aqueous zinc complexes and metallic zinc. *Geochim. Cosmochim. Acta* **2011**, *175*, 769−783.

(100) Li, X. F.; Liu, Y. Equilibrium Se isotope fractionation parameters: A first-principles study. *Earth Planet. Sci. Lett.* **2011**, *304*, 113−120.

(101) Sonke, J. E.; Sivry, Y.; Viers, J.; Freydier, R.; Dejonghe, L.; Andre, L.; Aggarwal, J. K.; Fontan, F.; Dupre, B. Historical variations in the isotopic composition of atmospheric zinc deposition from a zinc smelter. *Chem. Geol.* **2008**, *252*, 145−157.

(102) Mattielli, N.; Petit, J. C. J.; Deboudt, K.; Flament, P.; Perdrix, E.; Taillez, A.; Rimetz-Planchon, J.; Weis, D. Zn isotope study of atmospheric emissions and dry depositions within a 5km radius of a Pb-Zn refinery. *Atmos. Environ.* **2009**, *43*, 1265−1272.

(103) Larner, F.; Rehkämper, M. Evaluation of stable isotope tracing for ZnO nanomaterials − new constraints from high precision isotope analyses and modelling. *Environ. Sci. Technol.* **2012**, *46*, 4149−4158.

(104) Borrok, D. M.; Gieré, R.; Ren, M.; Landa, E. R. Zinc isotopic composition of particulate matter generated during the combustion of coal and coal+tire-derived fuels. *Environ. Sci. Technol.* **2010**, *44*, 9219−9224.

(105) Cloquet, C.; Carignan, J.; Libourel, G.; Sterckeman, T.; Perdrix, E. Tracing source pollution in soils using cadmium and lead isotopes. *Environ. Sci. Technol.* **2006**, *40*, 2525−2530.

(106) Shiel, A. E.; Weiss, D.; Orians, K. J. Evaluation of zinc, cadmium and lead isotope fractionation during smelting and refining. *Sci. Total Environ.* **2010**, *408*, 2357−2368.

(107) Sun, R.; Heimbürger, L.-E.; Sonke, J. E.; Liu, G.; Amouroux, D.; Berail, S. Mercury stable isotope fractionation in six utility boilers of two large coal-fired power plants. *Chem. Geol.* **2013**, *336*, 103−111.

(108) Wiederhold, J. G.; Smith, R. S.; Siebner, H.; Jew, A. D.; Brown, G. E.; Bourdon, B.; Kretzschmar, R. Mercury isotope signatures as tracers for Hg cycling at the New Idria Hg Mine. *Environ. Sci. Technol.* **2013**, *47*, 6137−6145.

DOI: 10.1021/es504683e
Environ. Sci. Technol. 2015, 49, 2606−2624

(109) Black, J. R.; Umeda, G.; Dunn, B.; McDonough, W. F.; Kavner, A. The electrochemical isotope effect and lithium isotope separation. *J. Am. Chem. Soc.* **2009**, *131*, 9904−9905.
(110) Kavner, A.; Shahar, A.; Black, J. R.; Young, E. Iron isotope electroplating: Diffusion-limited fractionation. *Chem. Geol.* **2009**, *267*, 131−138.
(111) Kavner, A.; John, S. G.; Sass, S.; Boyle, E. A. Redox-driven stable isotope fractionation in transition metals: Application to Zn electroplating. *Geochim. Cosmochim. Acta* **2008**, *72*, 1731−1741.
(112) Dideriksen, K.; Baker, J. A.; Stipp, S. L. S. Equilibrium Fe isotope fractionation between inorganic aqueous Fe(III) and the siderophore complex, Fe(III)-desferrioxamine B. *Earth Planet. Sci. Lett.* **2008**, *269*, 280−290.
(113) Jouvin, D.; Louvat, P.; Juillot, F.; Marechal, C. N.; Benedetti, M. F. Zinc isotopic fractionation: Why organic matters. *Environ. Sci. Technol.* **2009**, *43*, 5747−5754.
(114) Ryan, B. M.; Kirby, J. K.; Degryse, F.; Scheiderich, K.; McLaughlin, M. J. Copper isotope fractionation during equilibration with natural and synthetic ligands. *Environ. Sci. Technol.* **2014**, *48*, 8620−8626.
(115) Bigalke, M.; Weyer, S.; Wilcke, W. Copper isotope fractionation during complexation with insolubilized humic acid. *Environ. Sci. Technol.* **2010**, *44*, 5496−5502.
(116) Morgan, J. L.; Wasylenki, L. E.; Nuester, J.; Anbar, A. D. Fe isotope fractionation during equilibration of Fe-organic complexes. *Environ. Sci. Technol.* **2010**, *44*, 6095−6101.
(117) Li, W.; Beard, B. L.; Li, C.; Johnson, C. M. Magnesium isotope fractionation between brucite [$Mg(OH)_2$] and Mg aqueous species: Implications for silicate weathering and biogeochemical processes. *Earth Planet. Sci. Lett.* **2014**, *394*, 82−93.
(118) Hill, P. S.; Schauble, E. A.; Shahar, A.; Tonui, E.; Young, E. D. Experimental studies of equilibrium iron isotope fractionation in ferric aquo-chloro complexes. *Geochim. Cosmochim. Acta* **2009**, *73*, 2366−2381.
(119) Nir, O.; Vengosh, A.; Harkness, J. S.; Dwyer, G. S.; Lahav, O. Direct measurement of the boron isotope fractionation factor: Reducing the uncertainty in reconstructing ocean paleo-pH. *Earth Planet. Sci. Lett.* **2015**, *414*, 1−5.
(120) Liu, Y.; Tossell, J. A. Ab initio molecular orbital calculations for boron isotope fractionations on boric acids and borates. *Geochim. Cosmochim. Acta* **2005**, *69*, 3995−4006.
(121) Domagal-Goldman, S. D.; Kubicki, J. D. Density functional theory predictions of equilibrium isotope fractionation of iron due to redox changes and organic complexation. *Geochim. Cosmochim. Acta* **2008**, *72*, 5201−5216.
(122) Domagal-Goldman, S. D.; Paul, K. W.; Sparks, D. L.; Kubicki, J. D. Quantum chemical study of the Fe(III)-desferrioxamine B siderophore complex: electronic structure, vibrational frequencies, and equilibrium Fe-isotope fractionation. *Geochim. Cosmochim. Acta* **2009**, *73*, 1−12.
(123) Ottonello, G.; Zuccolini, M. V. The iron-isotope fractionation dictated by the carboxylic functional: An ab-initio investigation. *Geochim. Cosmochim. Acta* **2008**, *72*, 5920−5934.
(124) Moynier, F.; Fujii, T.; Wang, K.; Foriel, J. Ab initio calculations of the Fe(II) and Fe(III) isotopic effects in citrates, nicotianamine, and phytosiderophore, and new Fe isotopic measurements in higher plants. *C. R. Geoscience* **2013**, *345*, 230−240.
(125) Fujii, T.; Moynier, F.; Blichert-Toft, J.; Albarède, F. Density functional theory estimation of isotope fractionation of Fe, Ni, Cu, and Zn among species relevant to geochemical and biological environments. *Geochim. Cosmochim. Acta* **2014**, *140*, 553−576.
(126) Seo, J.; Lee, S.; Lee, I. Quantum chemical calculations of equilibrium copper (I) isotope fractionations in ore-forming fluids. *Chem. Geol.* **2007**, *243*, 225−237.
(127) Fujii, T.; Albarède, F. Ab Initio calculation of the Zn isotope effect in phosphates, citrates, and malates and applications to plants and soil. *PLoS One* **2012**, *7* (2), e30726.
(128) Fujii, T.; Moynier, F.; Pons, M.; Albarède, F. The origin of Zn isotope fractionation in sulfides. *Geochim. Cosmochim. Acta* **2011**, *75*, 7632−7643.
(129) Li, X.; Zhao, H.; Tang, M.; Liu, Y. Theoretical prediction for several important equilibrium Ge isotope fractionation factors and geological implications. *Earth Planet. Sci. Lett.* **2009**, *287*, 1−11.
(130) Tossell, J. A. Calculating the partitioning of the isotopes of Mo between oxidic and sulfidic species in aqueous solution. *Geochim. Cosmochim. Acta* **2005**, *69*, 2981−2993.
(131) Yang, J.; Li, Y.; Liu, S.; Tian, H.; Chen, C.; Liu, J.; Shi, Y. Theoretical calculations of Cd isotope fractionation in hydrothermal fluids. *Chem. Geol.* **2015**, *391*, 74−82.
(132) Barling, J.; Anbar, A. D. Molybdenum isotope fractionation during adsorption by manganese oxides. *Earth Planet. Sci. Lett.* **2004**, *217*, 315−329.
(133) Wasylenki, L. E.; Weeks, C. L.; Bargar, J. R.; Spiro, T. G.; Hein, J. R.; Anbar, A. D. The molecular mechanism of Mo isotope fractionation during adsorption to birnessite. *Geochim. Cosmochim. Acta* **2011**, *75*, 5019−5031.
(134) Balistrieri, L. S.; Borrok, D. M.; Wanty, R. B.; Ridley, W. I. Fractionation of Cu and Zn isotopes during adsorption onto amorphous Fe(III) oxyhydroxide: Experimental mixing of acid rock drainage and ambient river water. *Geochim. Cosmochim. Acta* **2008**, *72*, 311−328.
(135) Pokrovsky, O. S.; Galy, A.; Schott, J.; Pokrovski, G. S.; Mantoura, S. Germanium isotope fractionation during Ge adsorption on goethite and its coprecipitation with Fe oxy(hydr)oxides. *Geochim. Cosmochim. Acta* **2014**, *131*, 138−149.
(136) Mitchell, K.; Couture, R.-M.; Johnson, T. M.; Mason, P. R. D.; Van Cappellen, P. Selenium sorption and isotope fractionation: Iron(III) oxides versus iron(II) sulfides. *Chem. Geol.* **2013**, *342*, 21−28.
(137) Brennecka, G. A.; Wasylenki, L. E.; Bargar, J. R.; Weyer, S.; Anbar, A. D. Uranium isotope fractionation during adsorption to Mn oxyhydroxides. *Environ. Sci. Technol.* **2011**, *45*, 1370−1375.
(138) Ockert, C.; Gussone, N.; Kaufhold, S.; Teichert, B. M. A. Isotope fractionation during Ca exchange on clay minerals in a marine environment. *Geochim. Cosmochim. Acta* **2013**, *112*, 374−388.
(139) Li, D.; Liu, S. A.; Li, S. Copper isotope fractionation during adsorption onto kaolinite: Experimental approach and applications. *Chem. Geol.* **2015**, *396*, 74−82.
(140) Wasylenki, L. E.; Swihart, J. W.; Romaniello, S. J. Cadmium isotope fractionation during adsorption to Mn oxyhydroxide at low and high ionic strength. *Geochim. Cosmochim. Acta* **2014**, *140*, 212−226.
(141) Goldberg, T.; Archer, C.; Vance, D.; Poulton, S. Mo isotope fractionation during adsorption to Fe (oxyhydr)oxides. *Geochim. Cosmochim. Acta* **2009**, *73*, 6502−6516.
(142) Lemarchand, E.; Schott, J.; Gaillardet, J. How surface complexes impact boron isotope fractionation: evidence from Fe and Mn oxides sorption experiments. *Earth Planet. Sci. Lett.* **2007**, *260*, 277−296.
(143) Pokrovsky, O. S.; Viers, J.; Freydier, R. Zinc stable isotope fractionation during its adsorption on oxides and hydroxides. *J. Colloid Interface Sci.* **2005**, *291*, 192−200.
(144) Nakada, R.; Tanimizu, M.; Takahashi, Y. Difference in the stable isotopic fractionations of Ce, Nd, and Sm during adsorption on iron and manganese oxides and its interpretation based on their local structures. *Geochim. Cosmochim. Acta* **2013**, *121*, 105−119.
(145) Mikutta, C.; Wiederhold, J. G.; Cirpka, O. A.; Hofstetter, T. B.; Bourdon, B.; Von Gunten, U. Iron isotope fractionation and atom exchange during sorption of ferrous iron to mineral surfaces. *Geochim. Cosmochim. Acta* **2009**, *73*, 1795−1812.
(146) Beard, B. L.; Handler, R. M.; Scherer, M. M.; Wu, L. L.; Czaja, A. D.; Heimann, A.; Johnson, C. M. Iron isotope fractionation between aqueous ferrous iron and goethite. *Earth Planet. Sci. Lett.* **2010**, *295*, 241−250.
(147) Nakada, R.; Takahashi, Y.; Tanimizu, M. Isotopic and speciation study on cerium during its solid−water distribution with

implication for Ce stable isotope as a paleo-redox proxy. *Geochim. Cosmochim. Acta* **2013**, *103*, 49−62.

(148) Nielsen, S. G.; Wasylenki, L. E.; Rehkämper, M.; Peacock, C. L.; Xue, Z.; Moon, E. M. Towards an understanding of thallium isotope fractionation during adsorption to manganese oxides. *Geochim. Cosmochim. Acta* **2013**, *117*, 252−265.

(149) Pokrovsky, O. S.; Viers, J.; Emnova, E. E.; Kompantseva, E. I.; Freydier, R. Copper isotope fractionation during its interaction with soil and aquatic microorganisms and metal oxy(hydr)oxides: Possible structural control. *Geochim. Cosmochim. Acta* **2008**, *72*, 1742−1757.

(150) Navarrete, J. U.; Borrok, D. M.; Viveros, M.; Ellzey, J. T. Copper isotope fractionation during surface adsorption and intracellular incorporation by bacteria. *Geochim. Cosmochim. Acta* **2011**, *75*, 784−799.

(151) Kafantaris, F-C. A.; Borrok, D. M. Zinc isotope fractionation during surface adsorption and intracellular incorporation by bacteria. *Chem. Geol.* **2014**, *366*, 42−51.

(152) Coutaud, A.; Meheut, M.; Viers, J.; Rols, J. L.; Pokrovsky, O. S. Zn isotope fractionation during interaction with phototrophic biofilm. *Chem. Geol.* **2014**, *390*, 46−60.

(153) Little, S. H.; Sherman, D. M.; Vance, D.; Hein, J. R. Molecular controls on Cu and Zn isotopic fractionation in Fe−Mn crusts. *Earth Planet. Sci. Lett.* **2014**, *396*, 213−222.

(154) Juillot, F.; Marechal, C.; Ponthieu, M.; Cacaly, S.; Morin, G.; Benedetti, M.; Hazemann, J. L.; Proux, O.; Guyot, F. Zn isotopic fractionation caused by sorption on goethite and 2-lines ferrihydrite. *Geochim. Cosmochim. Acta* **2008**, *72*, 4886−4900.

(155) Kashiwabara, T.; Takahashi, Y.; Tanimizu, M. A XAFS study on the mechanism of isotopic fractionation of molybdenum during its adsorption on ferromanganese oxides. *Geochem. J.* **2009**, *43*, e31−e36.

(156) Li, X. F.; Liu, Y. First-principles study of Ge isotope fractionation during adsorption onto Fe(III)-oxyhydroxide surfaces. *Chem. Geol.* **2010**, *278*, 15−22.

(157) Ellis, A.; Johnson, T. M.; Bullen, T. D. Using chromium stable isotope ratios to quantify Cr(VI) reduction: lack of sorption effects. *Environ. Sci. Technol.* **2004**, *38*, 3604−3607.

(158) Shiel, A. E.; Laubach, P. G.; Johnson, T. M.; Lundstrom, C. C.; Long, P. E.; Williams, K. H. No measurable changes in $^{238}U/^{235}U$ due to desorption−adsorption of U(VI) from groundwater at the Rifle, Colorado, integrated field research challenge site. *Environ. Sci. Technol.* **2013**, *47*, 2535−2541.

(159) Oelze, M.; von Blanckenburg, F.; Hoellen, D.; Dietzel, M.; Bouchez, J. Si stable isotope fractionation during adsorption and the competition between kinetic and equilibrium isotope fractionation: Implications for weathering systems. *Chem. Geol.* **2014**, *380*, 161−171.

(160) Jiskra, M.; Saile, D.; Wiederhold, J. G.; Bourdon, B.; Björn, E.; Kretzschmar, R. Kinetics of Hg(II) exchange between organic ligands, goethite, and natural organic matter studied with an enriched stable isotope approach. *Environ. Sci. Technol.* **2014**, *48*, 13207−13217.

(161) DePaolo, D. J. Surface kinetic model for isotopic and trace element fractionation during precipitation of calcite from aqueous solutions. *Geochim. Cosmochim. Acta* **2011**, *75*, 1039−1056.

(162) Matsuhisa, Y.; Goldsmith, J. R.; Clayton, R. N. Mechanisms of hydrothermal crystallization of quartz at 250°C and 15 kbar. *Geochim. Cosmochim. Acta* **1978**, *42*, 173−182.

(163) Butler, I. B.; Archer, C.; Vance, D.; Oldroyd, A.; Rickard, D. Fe isotope fractionation on FeS formation in ambient aqueous solution. *Earth Planet. Sci. Lett.* **2005**, *236*, 430−442.

(164) Guilbaud, R.; Butler, I. B.; Ellam, R. M.; Rickard, D.; Oldroyd, A. Experimental determination of the equilibrium Fe isotope fractionation between Fe^{2+}_{aq} and FeS_m (mackinawite) at 25 and 2°C. *Geochim. Cosmochim. Acta* **2011**, *75*, 2721−2734.

(165) Wu, L.; Druschel, G.; Findlay, A.; Beard, B. L.; Johnson, C. M. Experimental determination of iron isotope fractionations among Fe_{aq}^{2+}-FeS_{aq}-Mackinawite at low temperatures: implications for the rock record. *Geochim. Cosmochim. Acta* **2012**, *89*, 46−61.

(166) Marriott, C. S.; Henderson, G. M.; Belshaw, N. S.; Tudhope, A. W. Temperature dependence of δ^7Li, δ^{44}Ca and Li/Ca during growth of calcium carbonate. *Earth Planet. Sci. Lett.* **2004**, *222*, 615−624.

(167) Wimpenny, J.; Gislason, S.; James, R. H.; Gannoun, A.; Pogge von Strandmann, P. A. E.; Burton, K. W. The behaviour of Li and Mg isotopes during primary phase dissolution and secondary mineral formation in basalt. *Geochim. Cosmochim. Acta* **2010**, *74*, 5259−5279.

(168) Immenhauser, A.; Buhl, D.; Richter, D.; Niedermayr, A.; Riechelmann, D.; Dietzel, M.; Schulte, U. Magnesium-isotope fractionation during low-Mg calcite precipitation in a limestone cave—Field study and experiments. *Geochim. Cosmochim. Acta* **2010**, *74*, 4346−4364.

(169) Mavromatis, V.; Pearce, C. R.; Shirokova, L. S.; Bundeleva, I. A.; Pokrovsky, O. S.; Benezeth, P.; Oelkers, E. H. Magnesium isotope fractionation during hydrous magnesiumcarbonate precipitation with and without cyanobacteria. *Geochim. Cosmochim. Acta* **2012**, *76*, 161−174.

(170) Li, W.; Chakraborty, S.; Beard, B. L.; Romanek, C. S.; Johnson, C. M. Magnesium isotope fractionation during precipitation of inorganic calcite under laboratory conditions. *Earth Planet. Sci. Lett.* **2012**, *333*−*334*, 304−316.

(171) Saulnier, S.; Rollion-Bard, C.; Vigier, N.; Chaussidon, M. Mg isotope fractionation during calcite precipitation: An experimental study. *Geochim. Cosmochim. Acta* **2012**, *91*, 75−91.

(172) Pearce, C. R.; Saldi, G. D.; Schott, J.; Oelkers, E. H. Isotopic fractionation during congruent dissolution, precipitation and at equilibrium: Evidence from Mg isotopes. *Geochim. Cosmochim. Acta* **2012**, *92*, 170−183.

(173) Gussone, N.; Eisenhauer, A.; Heuser, A.; Dietzel, M.; Bock, B.; Böhm, F.; Spero, H. J.; Lea, D.; Bijma, J.; Nägler, T. Model of kinetic effects on calcium isotope fractionation (δ^{44}Ca) in inorganic aragonite and cultured planktonic foraminifera. *Geochim. Cosmochim. Acta* **2003**, *67*, 1375−1382.

(174) Lemarchand, D.; Wasserburg, G. J.; Papanastassiou, D. A. Rate-controlled calcium isotope fractionation in synthetic calcite. *Geochim. Cosmochim. Acta* **2004**, *68*, 4665−4678.

(175) Tang, J.; Dietzel, M.; Böhm, F.; Köhler, S. J.; Eisenhauer, A. Sr^{2+}/Ca^{2+} and $^{44}Ca/^{40}Ca$ fractionation during inorganic calcite formation: II. Ca isotopes. *Geochim. Cosmochim. Acta* **2008**, *72*, 3733−3745.

(176) Gussone, N.; Nehrke, G.; Teichert, B. M. A. Calcium isotope fractionation in ikaite and vaterite. *Chem. Geol.* **2011**, *285*, 194−202.

(177) Böhm, F.; Eisenhauer, A.; Tang, J.; Dietzel, M.; Krabbenhoft, A.; Kisakurek, B.; Horn, C. Strontium isotope fractionation of planktic foraminifera and inorganic calcite. *Geochim. Cosmochim. Acta* **2012**, *93*, 300−314.

(178) von Allmen, K.; Böttcher, M. E.; Samankassou, E.; Nägler, T. F. Barium isotope fractionation in the global barium cycle: First evidence from barium minerals and precipitation experiments. *Chem. Geol.* **2010**, *277*, 70−77.

(179) Böttcher, M. E.; Geprägs, P.; Neubert, N.; von Allmen, K.; Pretet, C.; Samankassou, E.; Nägler, T. F. Barium isotope fractionation during experimental formation of the double carbonate $BaMn[CO_3]_2$ at ambient temperature. *Isotopes Environ. Health Stud.* **2012**, *48*, 457−463.

(180) Wiesli, R. A.; Beard, B. L.; Johnson, C. M. Experimental determination of Fe isotope fractionation between aqueous Fe(II), siderite and "green rust" in abiotic systems. *Chem. Geol.* **2004**, *211*, 343−362.

(181) Griffith, E. M.; Schauble, E. A.; Bullen, T. D.; Paytan, A. Characterization of calcium isotopes in natural and synthetic barite. *Geochim. Cosmochim. Acta* **2008**, *72*, 5641−5658.

(182) Harouaka, K.; Eisenhauer, A.; Fantle, M. S. Experimental investigation of Ca isotopic fractionation during abiotic gypsum precipitation. *Geochim. Cosmochim. Acta* **2014**, *129*, 157−176.

(183) Li, W.; Beard, B. L.; Johnson, C. M. Exchange and fractionation of Mg isotopes between epsomite and saturated $MgSO_4$ solution. *Geochim. Cosmochim. Acta* **2011**, *75*, 1814−1828.

(184) Widanagamage, I. H.; Schauble, E. A.; Scher, H. D.; Griffith, E. M. Stable strontium isotope fractionation in synthetic barite. *Geochim. Cosmochim. Acta* **2014**, *147*, 58−75.

DOI: 10.1021/es504683e
Environ. Sci. Technol. 2015, 49, 2606−2624

(185) Bullen, T. D.; White, A. F.; Childs, C. W.; Vivit, D. V.; Schulz, M. S. Demonstration of significant abiotic iron isotope fractionation in nature. *Geology* **2001**, *29*, 699−702.
(186) Skulan, J. L.; Beard, B. L.; Johnson, C. M. Kinetic and equilibrium Fe isotope fractionation between aqueous Fe(III) and hematite. *Geochim. Cosmochim. Acta* **2002**, *66*, 2995−3015.
(187) Balci, N.; Bullen, T. D.; Witte-Lien, K.; Shanks, W. C.; Motelica, M.; Mandernack, K. W. Iron isotope fractionation during microbially stimulated Fe(II) oxidation and Fe(III) precipitation. *Geochim. Cosmochim. Acta* **2006**, *70*, 622−639.
(188) Saunier, G.; Pokrovski, G. S.; Poitrasson, F. First experimental determination of iron isotope fractionation between hematite and aqueous solution at hydrothermal conditions. *Geochim. Cosmochim. Acta* **2011**, *75*, 6629−6654.
(189) Guilbaud, R.; Butler, I. B.; Ellam, R. M. Abiotic pyrite formation produces a large Fe isotope fractionation. *Science* **2011**, *332*, 1548−1551.
(190) Syverson, D. D.; Borrok, D. M.; Seyfried, W. E., Jr. Experimental determination of equilibrium Fe isotopic fractionation between pyrite and dissolved Fe under hydrothermal conditions. *Geochim. Cosmochim. Acta* **2013**, *122*, 170−183.
(191) Foucher, D.; Hintelmann, H.; Al, T. A.; MacQuarrie, K. T. Mercury isotope fractionation in waters and sediments of the Murray Brookmine watershed (New Brunswick, Canada): Tracing mercury contamination and transformation. *Chem. Geol.* **2013**, *336*, 87−95.
(192) Luo, Y.; Celo, V.; Dabek-Zlotorzynska, E.; Yang, L. Effects of precipitation and UV photolysis on Ag isotope ratio: Experimental studies. *J. Anal. At. Spectrom.* **2012**, *27*, 299−304.
(193) Geilert, S.; Vroon, P. Z.; Roerdink, D. L.; Cappellen, P. V.; van Bergen, M. J. Silicon isotope fractionation during abiotic silica precipitation at low temperatures: Inferences from flow-through experiments. *Geochim. Cosmochim. Acta* **2014**, *142*, 95−114.
(194) Oelze, M.; von Blanckenburg, F.; Bouchez, J.; Hoellen, D.; Dietzel, M. The effect of Al on Si isotope fractionation investigated by silica precipitation experiments. *Chem. Geol.* **2015**, *397*, 94−105.
(195) Vigier, N.; Decarreau, A.; Millot, R.; Carignan, J.; Petit, S.; France-Lanord, C. Quantifying Li isotope fractionation during smectite formation and implications for the Li cycle. *Geochim. Cosmochim. Acta* **2008**, *72*, 780−792.
(196) Wimpenny, J.; Colla, C. A.; Yin, Q.-Z.; Rustad, J. R.; Casey, W. H. Investigating the behaviour of Mg isotopes during the formation of clay minerals. *Geochim. Cosmochim. Acta* **2014**, *128*, 178−194.
(197) Schauble, E. A. First-principles estimates of equilibrium magnesium fractionation in silicate, oxide, carbonate and hexaaquamagnesium(2+) crystals. *Geochim. Cosmochim. Acta* **2011**, *75*, 844−869.
(198) Rustad, J. R.; Casey, W. H.; Yin, Q.-Z.; Bylaska, E. J.; Felmy, A. R.; Bogatko, S. A.; Jackson, V. E.; Dixon, D. A. Isotopic fractionation of Mg^{2+}(aq), Ca^{2+}(aq), and Fe^{2+}(aq) with carbonate minerals. *Geochim. Cosmochim. Acta* **2010**, *74*, 6301−6323.
(199) Méheut, M.; Schauble, E. A. Silicon isotope fractionation in silicate minerals: Insights from first-principles models of phyllosilicates, albite and pyrope. *Geochim. Cosmochim. Acta* **2014**, *134*, 137−154.
(200) Dupuis, R.; Benoit, M.; Nardin, E.; Méheut, M. Fractionation of silicon isotopes in liquids: the importance of configurational disorder. *Chem. Geol.* **2015**, *396*, 239−254.
(201) Colla, C. A.; Wimpenny, J.; Yin, Q.-Z.; Rustad, J. R.; Casey, W. H. Calcium-isotope fractionation between solution and solids with six, seven or eight oxygens bound to Ca(II). *Geochim. Cosmochim. Acta* **2014**, *121*, 363−373.
(202) Polyakov, V. B.; Clayton, R. N.; Horita, J.; Mineev, S. D. Equilibrium iron isotope fractionation factors of minerals: Reevaluation from the data of nuclear inelastic resonant X-ray scattering and Mössbauer spectroscopy. *Geochim. Cosmochim. Acta* **2007**, *71*, 3833−3846.
(203) Blanchard, M.; Poitrasson, F.; Méheut, M.; Lazzeri, M.; Mauri, F.; Balan, E. Iron isotope fractionation between pyrite (FeS_2), hematite (Fe_2O_3) and siderite ($FeCO_3$): a first-principles density functional theory study. *Geochim. Cosmochim. Acta* **2009**, *72*, 6565−6578.
(204) Dauphas, N.; Roskosz, M.; Alp, E. E.; Golden, D. C.; Sio, C. K.; Tissot, F. L. H.; Hu, M. Y.; Zhao, J.; Gao, L.; Morris, R. V. A general moment NRIXS approach to the determination of equilibrium Fe isotopic fractionation factors: Application to goethite and jarosite. *Geochim. Cosmochim. Acta* **2012**, *94*, 254−275.
(205) Hofmann, A. E.; Bourg, I. C.; DePaolo, D. J. Ion desolvation as a mechanism for kinetic isotope fractionation in aqueous systems. *Proc. Natl. Acad. Sci. U. S. A.* **2012**, *109*, 18689−18694.
(206) Wiederhold, J. G.; Kraemer, S. M.; Teutsch, N.; Borer, P. M.; Halliday, A. N.; Kretzschmar, R. Iron isotope fractionation during proton-promoted, ligand-controlled, and reductive dissolution of goethite. *Environ. Sci. Technol.* **2006**, *40*, 3787−3793.
(207) Kiczka, M.; Wiederhold, J. G.; Frommer, J.; Voegelin, A.; Kraemer, S. M.; Bourdon, B.; Kretzschmar, R. Iron speciation and isotope fractionation during silicate weathering and soil formation in an alpine glacier forefield chronosequence. *Geochim. Cosmochim. Acta* **2011**, *75*, 5559−5573.
(208) Voinot, A.; Lemarchand, D.; Collignon, C.; Granet, M.; Chabaux, F.; Turpault, M.-P. Experimental dissolution vs. transformation of micas under acidic soil conditions: Clues from boron isotopes. *Geochim. Cosmochim. Acta* **2013**, *117*, 144−160.
(209) Ryu, J. S.; Jacobson, A. D.; Holmden, C.; Lundstrom, C.; Zhang, Z. The major ion, $\delta^{44/40}$Ca, $\delta^{44/42}$Ca, and $\delta^{26/24}$Mg geochemistry of granite weathering at pH = 1 and T = 25°C: power-law processes and the relative reactivity of minerals. *Geochim. Cosmochim. Acta* **2011**, *75*, 6004−6026.
(210) Brantley, S. L.; Liermann, L.; Bullen, T. D. Fractionation of Fe isotopes by soil microbes and organic acids. *Geology* **2001**, *29*, 535−538.
(211) Brantley, S. L.; Liermann, L. J.; Guynn, R. L.; Anbar, A.; Icopini, G. A.; Barling, J. Fe isotopic fractionation during mineral dissolution with and without bacteria. *Geochim. Cosmochim. Acta* **2004**, *68*, 3189−3204.
(212) Chapman, J. B.; Weiss, D. J.; Shan, Y.; Lemberger, M. Iron isotope fractionation during leaching of granite and basalt by hydrochloric and oxalic acids. *Geochim. Cosmochim. Acta* **2009**, *73*, 1312−1324.
(213) Kiczka, M.; Wiederhold, J. G.; Frommer, J.; Kraemer, S. M.; Bourdon, B.; Kretzschmar, R. Iron isotope fractionation during proton- and ligand-promoted dissolution of primary phyllosilicates. *Geochim. Cosmochim. Acta* **2010**, *74*, 3112−3128.
(214) Weiss, D. J.; Boye, K.; Caldelas, C.; Fendorf, S. Zinc isotope fractionation during early dissolution of biotite granite. *Soil Sci. Soc. Am. J.* **2014**, *78*, 171−179.
(215) Demarest, M. S.; Brzezinski, M. A.; Beucher, C. P. Fractionation of silicon isotopes during biogenic silica dissolution. *Geochim. Cosmochim. Acta* **2009**, *73*, 5572−5583.
(216) Wetzel, F.; de Souza, G. F.; Reynolds, B. C. What controls silicon isotope fractionation during dissolution of diatom opal? *Geochim. Cosmochim. Acta* **2014**, *131*, 128−137.
(217) Cobert, F.; Schmitt, A. D.; Calvaruso, C.; Turpault, M. P.; Lemarchand, D.; Collignon, C.; Chabaux, F.; Stille, P. Biotic and abiotic experimental identification of bacterial influence on calcium isotopic signatures. *Rapid Commun. Mass Spectrom.* **2011**, *25*, 2760−2768.
(218) Fernandez, A.; Borrok, D. M. Fractionation of Cu, Fe and Zn isotopes during the oxidative weathering of sulfide rich rocks. *Chem. Geol.* **2009**, *264*, 1−12.
(219) Mathur, R.; Ruiz, J.; Titley, S.; Liermann, L.; Buss, H.; Brantley, S. Cu isotopic fractionation in the supergene environment with and without bacteria. *Geochim. Cosmochim. Acta* **2005**, *69*, 5233−5246.
(220) Kimball, B. E.; Mathur, R.; Dohnalkova, A. C.; Wall, A. J.; Runkel, R. L.; Brantley, S. L. Copper isotope fractionation in acid mine drainage. *Geochim. Cosmochim. Acta* **2009**, *73*, 1247−1263.
(221) Wall, A. J.; Mathur, R.; Post, J. E.; Heaney, P. J. Cu isotope fractionation during bornite dissolution: An in situ X-ray diffraction analysis. *Ore Geol. Rev.* **2011**, *42*, 62−70.

DOI: 10.1021/es504683e
Environ. Sci. Technol. 2015, 49, 2606−2624

(222) Matthies, R.; Krahé, L.; Blowes, D. W. Zinc stable isotope fractionation upon accelerated oxidative weathering of sulfidic mine waste. *Sci. Total Environ.* **2014**, *487*, 97−101.
(223) Rodríguez, N. P.; Khoshkhoo, M.; Sandström, Å; Rodushkin, I.; Alakangas, L.; Öhlander, B. Isotopic signature of Cu and Fe during bioleaching and electrochemical leaching of a chalcopyrite concentrate. *Int. J. Miner. Proc.* **2015**, *134*, 58−65.
(224) Richter, F. M.; Dauphas, N.; Teng, F.-Z. Non-traditional fractionation of nontraditional isotopes: evaporation, chemical diffusion and Soret diffusion. *Chem. Geol.* **2009**, *258*, 92−103.
(225) Brönsted, J. N.; von Hevesy, G. Über die Trennung der Isotopen des Quecksilbers. *Z. Phys. Chem.* **1921**, *99*, 189−206.
(226) Mulliken, R. S.; Harkins, W. D. The separation of isotopes. Theory of resolution of isotopic mixtures by diffusion and similar processes. Experimental separation of mercury by evaporation in a vacuum. *J. Am. Chem. Soc.* **1922**, *44*, 37−65.
(227) Estrade, N.; Carignan, J.; Sonke, J. E.; Donard, O. F. X. Mercury isotope fractionation during liquid−vapor evaporation experiments. *Geochim. Cosmochim. Acta* **2009**, *73*, 2693−2711.
(228) Ghosh, S.; Schauble, E. A.; Lacrampe Couloume, G.; Blum, J. D.; Bergquist, B. A. Estimation of nuclear volume dependent fractionation of mercury isotopes in equilibrium liquid−vapor evaporation experiments. *Chem. Geol.* **2013**, *336*, 5−12.
(229) Davis, A. M.; Hashimoto, A.; Clayton, R. N.; Mayeda, T. K. Isotope mass fractionation during evaporation of Mg_2SiO_4. *Nature* **1990**, *347*, 655−658.
(230) Zhang, J.; Huang, S.; Davis, A. M.; Dauphas, N.; Hashimoto, A.; Jacobsen, S. B. Calcium and titanium isotopic fractionations during evaporation. *Geochim. Cosmochim. Acta* **2014**, *140*, 365−380.
(231) Wombacher, F.; Rehkamper, M.; Mezger, K. Determination of the mass-dependence of cadmium isotope fractionation during evaporation. *Geochim. Cosmochim. Acta* **2004**, *68*, 2349−2357.
(232) Lacks, D. J.; Goel, G.; Bopp, C. J.; Van Orman, J. A.; Lesher, C. E.; Lundstrom, C. C. Isotope fractionation by thermal diffusion in silicate melts. *Phys. Rev. Lett.* **2012**, *108*, 065901.
(233) Rodushkin, I.; Stenberg, A.; Andrén, H.; Malinovsky, D.; Baxter, D. C. Isotopic fractionation during diffusion of transition metal ions in solution. *Anal. Chem.* **2004**, *76*, 2148−2151.
(234) Malinovsky, D.; Baxter, D. C.; Rodushkin, I. Ion-specific isotopic fractionation of molybdenum during diffusion in aqueous solutions. *Environ. Sci. Technol.* **2007**, *41*, 1596−1600.
(235) Koster van Groos, P. G.; Esser, B. K.; Williams, R. W.; Hunt, J. R. Isotope effect of mercury diffusion in air. *Environ. Sci. Technol.* **2014**, *48*, 227−233.
(236) Eggenkamp, H. G. M.; Coleman, M. L. The effect of aqueous diffusion on the fractionation of chlorine and bromine stable isotopes. *Geochim. Cosmochim. Acta* **2009**, *73*, 3539−3548.
(237) Tyroller, L.; Brennwald, M. S.; Mächler, L.; Livingstone, D. M.; Kipfer, R. Fractionation of Ne and Ar isotopes by molecular diffusion in water. *Geochim. Cosmochim. Acta* **2014**, *136*, 60−66.
(238) Beard, B. L.; Johnson, C. M.; Cox, L.; Sun, H.; Nealson, K. H.; Aguilar, C. Iron isotope biosignatures. *Science* **1999**, *285*, 1889−1892.
(239) Ader, M.; Chaudhuri, S.; Coates, J. D.; Coleman, M. Microbial perchlorate reduction: A precise laboratory determination of the chlorine isotope fractionation and its possible biochemical basis. *Earth Planet Sci. Lett.* **2008**, *269*, 604−612.
(240) Crosby, H. A.; Roden, E. E.; Johnson, C. M.; Beard, B. L. The mechanisms of iron isotope fractionation produced during dissimilatory Fe(III) reduction by Shewanella putrefaciens and Geobacter sulfurreducens. *Geobiology* **2007**, *5*, 169−189.
(241) Sikora, E. R.; Johnson, T. M.; Bullen, T. D. Microbial mass-dependent fractionation of chromium isotopes. *Geochim. Cosmochim. Acta* **2008**, *72*, 3631−3641.
(242) Han, R.; Qin, L.; Brown, S. T.; Christensen, J. N.; Beller, H. R. Differential isotopic fractionation during Cr(VI) reduction by an aquifer-derived bacterium under aerobic versus denitrifying conditions. *Appl. Environ. Microbiol.* **2012**, *78*, 2462−2464.
(243) Basu, A.; Johnson, T. M.; Sanford, R. A. Cr isotope fractionation factors for Cr(VI) reduction by a metabolically diverse group of bacteria. *Geochim. Cosmochim. Acta* **2014**, *142*, 349−361.
(244) Herbel, M. J.; Johnson, T. M.; Oremland, R. S.; Bullen, T. D. Fractionation of selenium isotopes during bacterial respiratory reduction of selenium oxyanions. *Geochim. Cosmochim. Acta* **2000**, *64*, 3701−3709.
(245) Basu, A.; Sanford, R. A.; Johnson, T. M.; Lundstrom, C. C.; Löffler, F. E. Uranium isotope fractionation factors during U(VI) reduction by bacterial isolates. *Geochim. Cosmochim. Acta* **2014**, *136*, 100−113.
(246) Croal, L. R.; Johnson, C. M.; Beard, B. L.; Newman, D. K. 2004. Iron isotope fractionation by Fe(II)-oxidizing photoautotrophic bacteria. *Geochim. Cosmochim. Acta* **2004**, *68*, 1227−1242.
(247) Kappler, A.; Johnson, C. M.; Crosby, H. A.; Beard, B. L.; Newman, D. K. Evidence for equilibrium iron isotope fractionation by nitrate-reducing iron(II)-oxidizing bacteria. *Geochim. Cosmochim. Acta* **2010**, *74*, 2826−2842.
(248) Schilling, K.; Johnson, T. M.; Wilcke, W. Isotope fractionation of selenium during fungal biomethylation by Alternaria alternata. *Environ. Sci. Technol.* **2011**, *45*, 2670−2676.
(249) Rodriguez-Gonzalez, P.; Epov, V. N.; Bridou, R.; Tessier, E.; Guyoneaud, R.; Monperrus, M.; Amouroux, D. Species-specfic stable isotope fractionation of mercury during Hg(II) methylation by an anaerobic bacteria (*Desulfobulbus propionicus*) under dark conditions. *Environ. Sci. Technol.* **2009**, *43*, 9183−9188.
(250) Perrot, V.; Bridou, R.; Pedrero, Z.; Guyoneaud, R.; Monperrus, M.; Amouroux, D. Identical Hg isotope mass dependent fractionation signature during methylation by sulfate-reducing bacteria in sulfate and sulfate-free environment. *Environ. Sci. Technol.* **2015**, *49*, 1365−1373.
(251) Kritee, K.; Blum, J. D.; Reinfelder, J. R.; Barkay, T. Microbial stable isotope fractionation of mercury: A synthesis of present understanding and future directions. *Chem. Geol.* **2013**, *336*, 13−25.
(252) Wasylenki, L. E.; Anbar, A. D.; Liermann, L. J.; Mathur, R.; Gordon, G. W.; Brantley, S. L. Isotope fractionation during microbial metal uptake measured by MC-ICP-MS. *J. Anal. At. Spectrom.* **2007**, *22*, 905−910.
(253) Cameron, V.; Vance, D.; Archer, C.; House, C. H. A biomarker based on the stable isotopes of nickel. *Proc. Natl. Acad. Sci. U. S. A.* **2009**, *106*, 10944−10948.
(254) John, S. G.; Geis, R. W.; Saito, M. A.; Boyle, E. A. Zinc isotope fractionation during high-affinity and low-affinity zinc transport by the marine diatom *Thalassiosira oceanica*. *Limnol. Oceanogr.* **2007**, *52*, 2710−2714.
(255) Horner, T. J.; Lee, R. B. Y.; Henderson, G. M.; Rickaby, R. E. M. Nonspecific uptake and homeostasis drive the oceanic cadmium cycle. *Proc. Natl. Acad. Sci. U. S. A.* **2013**, *110*, 2500−2505.
(256) von Blanckenburg, F.; von Wirén, N.; Guelke, M.; Weiss, D. J.; Bullen, T. D. Fractionation of metal stable isotopes by higher plants. *Elements* **2009**, *5*, 375−380.
(257) Schmitt, A.-D.; Vigier, N.; Lemarchand, D.; Millot, R.; Chabaux, F.; Stille, P. Processes controlling the stable isotope compositions of Li, B, Mg and Ca in plants, soils and waters: A review. *C. R. Geosci.* **2012**, *344*, 704−722.
(258) Rosner, M.; Pritzkow, W.; Vogl, J.; Voerkelius, S. Development and validation of a method to determine the boron isotopic composition of crop plants. *Anal. Chem.* **2011**, *83*, 2562−2568.
(259) Black, J. R.; Epstein, E.; Rains, W. D.; Yin, Q. Z.; Casey, W. H. Magnesium-isotope fractionation during plant growth. *Environ. Sci. Technol.* **2008**, *42*, 7831−7836.
(260) Bolou-Bi, B. E.; Vigier, N.; Leyval, C.; Poszwa, A. Experimental determination of magnesium isotope fractionation during higher plant growth. *Geochim. Cosmochim. Acta* **2010**, *74*, 2523−2537.
(261) Opfergelt, S.; Cardinal, D.; Henriet, C.; André, L.; Delvaux, B. Silicon isotope fractionation between plant parts in banana: In situ vs. in vitro. *J. Geochem. Explor.* **2006**, *88*, 224−227.
(262) Ding, T.; Tian, S.; Sun, L.; Wu, L.; Zhou, J.; Chen, Z. Silicon isotope fractionation between rice plants and nutrient solution and its

DOI: 10.1021/es504683e
Environ. Sci. Technol. 2015, 49, 2606−2624

significance to the study of the silicon cycle. *Geochim. Cosmochim. Acta* **2008**, *72*, 5600−5615.

(263) Sun, A.; Xu, Q.; Xu, S.; Shen, H.; Sun, J.; Zhang, Y. Separation and analysis of chlorine isotopes in higher plants. *Chem. Geol.* **2014**, *381*, 21−25.

(264) Cobert, F.; Schmitt, A. D.; Bourgeade, P.; Labolle, F.; Badot, P. M.; Chabaux, F.; Stille, P. Experimental identification of Ca isotopic fractionations in higher plants. *Geochim. Cosmochim. Acta* **2011**, *75*, 5467−5482.

(265) Hindshaw, R. S.; Reynolds, B. C.; Wiederhold, J. G.; Kiczka, M.; Kretzschmar, R.; Bourdon, B. Calcium isotope fractionation in alpine plants. *Biogeochem.* **2013**, *112*, 373−388.

(266) de Souza, G. F.; Reynolds, B. C.; Kiczka, M.; Bourdon, B. Evidence for mass-dependent isotopic fractionation of strontium in a glaciated granitic watershed. *Geochim. Cosmochim. Acta* **2010**, *74*, 2596−2614.

(267) Guelke, M.; von Blanckenburg, F. Fractionation of stable iron isotopes in higher plants. *Environ. Sci. Technol.* **2007**, *41*, 1896−1901.

(268) Kiczka, M.; Wiederhold, J. G.; Kraemer, S. M.; Bourdon, B.; Kretzschmar, R. Iron isotope fractionation during Fe uptake and translocation in alpine plants. *Environ. Sci. Technol.* **2010**, *44*, 6144−6150.

(269) Deng, T-H-B.; Cloquet, C.; Tang, Y.-T.; Sterckeman, T.; Echevarria, G.; Estrade, N.; Morel, J.-L.; Qiu, R. L. Nickel and zinc isotope fractionation in hyperaccumulating and non-accumulating plants. *Environ. Sci. Technol.* **2014**, *48*, 11926−11933.

(270) Jouvin, D.; Weiss, D. J.; Mason, T. F. M.; Bravin, M.; Louvat, P.; Zhao, F. J.; Ferec, F.; Hinsinger, P.; Benedetti, M. F. Stable isotopes of Cu and Zn in higher plants: Evidence for Cu reduction at the root surface and two conceptual models for isotope fractionation processes. *Environ. Sci. Technol.* **2012**, *46*, 2652−2660.

(271) Ryan, B. M.; Kirby, J. K.; Degryse, F.; Harris, H.; McLaughlin, M. J.; Scheiderich, K. Copper speciation and isotopic fractionation in plants: uptake and translocation mechanisms. *New Phytol.* **2013**, *199*, 367−378.

(272) Weiss, D. J.; Mason, T. F. D.; Zhao, F. J.; Kirk, G. J. D.; Coles, B. J.; Horstwood, M. S. A. Isotopic discrimination of zinc in higher plants. *New Phytol.* **2005**, *165*, 703−710.

(273) Smolders, E.; Versieren, L.; Dong, S.; Mattielli, N.; Weiss, D. J.; Petrov, I.; Degryse, F. Isotopic fractionation of Zn in tomato plants reveals the role of root exudates on Zn uptake. *Plant Soil* **2013**, *370*, 605−613.

(274) Morgan, J. L. L.; Skulan, J. L.; Gordon, G. W.; Romaniello, S. J.; Smith, S. M.; Anbar, A. D. Rapidly assessing changes in bone mineral balance using natural stable calcium isotopes. *Proc. Natl. Acad. Sci. U. S. A.* **2012**, *109*, 9989−9994.

(275) Martin, J. E.; Vance, D.; Balter, V. Magnesium stable isotope ecology using mammal tooth enamel. *Proc. Natl. Acad. Sci. U.S.A.* **2015**, *112*, 430−435.

(276) Walczyk, T.; von Blanckenburg, F. Natural iron isotope variations in human blood. *Science* **2002**, *295*, 2065−2067.

(277) Walczyk, T.; von Blanckenburg, F. Deciphering the iron isotope message of the human body. *Int. J. Mass Spectrom.* **2005**, *242*, 117−134.

(278) von Blanckenburg, F.; Noordmann, J.; Guelke-Stelling, M. The iron stable isotope fingerprint of the human diet. *J. Agric. Food Chem.* **2013**, *61*, 11893−11899.

(279) Jaouen, K.; Pons, M.-L.; Balter, V. Iron, copper and zinc isotopic fractionation up mammal trophic chains. *Earth Planet. Sci. Lett.* **2013**, *374*, 164−172.

(280) Balter, V.; Lamboux, A.; Zazzo, A.; Télouk, P.; Leverrier, Y.; Marvel, L.; Moloney, A. P.; Monahan, F. J.; Schmidt, O.; Albarède, F. Contrasting Fe, Cu, and Zn isotopic patterns in organs and body fluids of mice and sheep, with emphasis on cellular fractionation. *Metallomics* **2013**, *5*, 1470−1482.

(281) Costas-Rodríguez, M.; Van Heghe, L.; Vanhaecke, F. Evidence for a possible dietary effect on the isotopic composition of Zn in blood via isotopic analysis of food products by multi-collector ICP-mass spectrometry. *Metallomics* **2014**, *6*, 139−146.

(282) Larner, F.; Woodley, L. N.; Shousha, S.; Moyes, A.; Humphreys-Williams, E.; Strekopytov, S.; Halliday, A. N.; Rehkämper, M.; Coombes, R. C. Zinc isotopic compositions of breast cancer tissue. *Metallomics* **2015**, *7*, 107−112.

(283) Hayes, J. M. Fractionation of carbon and hydrogen isotopes in biosynthetic processes. *Rev. Mineral. Geochem.* **2001**, *43*, 225−277.

(284) Canfield, D. E. Biogeochemistry of sulfur isotopes. *Rev. Mineral. Geochem.* **2001**, *43*, 607−636.

(285) Farkaš, J.; Déjeant, A.; Novák, M.; Jacobsen, S. B. Calcium isotope constraints on the uptake and sources of Ca^{2+} in a base-poor forest: a new concept of combining stable ($\delta^{44/42}$Ca) and radiogenic (ε_{Ca}) signals. *Geochim. Cosmochim. Acta* **2011**, *75*, 7031−7046.

(286) Hindshaw, R. S.; Reynolds, B. C.; Wiederhold, J. G.; Kretzschmar, R.; Bourdon, B. Calcium isotopes in a proglacial weathering environment: Damma Glacier, Switzerland. *Geochim. Cosmochim. Acta* **2011**, *75*, 106−118.

(287) Wiederhold, J. G.; Teutsch, N.; Kraemer, S. M.; Halliday, A. N.; Kretzschmar, R. Iron isotope fractionation during pedogenesis in redoximorphic soils. *Soil Sci. Soc. Am. J.* **2007**, *71*, 1840−1850.

(288) Thapalia, A.; Borrok, D. M.; van Metre, P. C.; Musgrove, M.; Landa, E. Zn and Cu isotopes as tracers of anthropogenic contamination in a sediment core from an urban lake. *Environ. Sci. Technol.* **2010**, *44*, 1544−1550.

(289) El Azzi, D.; Viers, J.; Guiresse, M.; Probst, A.; Aubert, D.; Caparros, J.; Charles, F.; Guizien, K.; Probst, J. L. Origin and fate of copper in a small Mediterranean vineyard catchment: New insights from combined chemical extraction and δ^{65}Cu isotopic composition. *Sci. Total Environ.* **2013**, *463*, 91−101.

(290) Schilling, K.; Johnson, T. M.; Mason, P. R. D. A sequential extraction technique for mass-balanced stable selenium isotope analysis of soil samples. *Chem. Geol.* **2014**, *381*, 125−130.

(291) Wiederhold, J. G.; Skyllberg, U.; Drott, A.; Jiskra, M.; Jonsson, S.; Björn, E.; Bourdon, B.; Kretzschmar, R. Mercury isotope signatures in contaminated sediments as tracer for local industrial pollution sources. *Environ. Sci. Technol.* **2015**, *49*, 177−185.

(292) Smith, R. S.; Wiederhold, J. G.; Jew, A. D.; Brown, G. E., Jr.; Bourdon, B.; Kretzschmar, R. Stable Hg isotope signatures in creek sediments impacted by a former Hg mine. *Environ. Sci. Technol.* **2015**, *49*, 767−776.

(293) Wiederhold, J. G.; Teutsch, N.; Kraemer, S. M.; Halliday, A. N.; Kretzschmar, R. Iron isotope fractionation in oxic soils by mineral weathering and podzolization. *Geochim. Cosmochim. Acta* **2007**, *71*, 5821−5833.

(294) Rodriguez-Gonzalez, P.; Epov, V. N.; Pécheyran, C.; Amouroux, D.; Donard, O. F. X. Species-specific stable isotope analysis by the hyphenation of chromatographic techniques with MC-ICPMS. *Mass. Spec. Rev.* **2012**, *31*, 504−521.

(295) Bouchez, J.; von Blanckenburg, F.; Schuessler, J. A. Modeling novel stable isotope ratios in the weathering zone. *Am. J. Sci.* **2013**, *313*, 267−308.

(296) Wanner, C.; Druhan, J. L.; Amos, R. T.; Alt-Epping, P.; Steefel, C. I. Benchmarking the simulation of Cr isotope fractionation. *Comp. Geosci.* **2015**, DOI: 10.1007/s10596-014-9436-9.

(297) Wiederhold, J. G. *Iron Isotope Fractionation in Soils—From Phenomena to Process Identification*. PhD thesis, Department of Environmental Sciences, ETH Zurich, Switzerland, 2006, DOI: 10.3929/ethz-a-005275890.

DOI: 10.1021/es504683e
Environ. Sci. Technol. 2015, 49, 2606−2624